HARVESTING NATURAL ALGAL BLOOMS FOR CONCURRENT BIOFUEL PRODUCTION AND HYPOXIA MITIGATION

BY

CHIH-TING KUO

THESIS

Submitted in partial fulfillment of the requirements
for the degree of Master of Science in Agricultural and Biological Engineering
in the Graduate College of the
University of Illinois at Urbana-Champaign, 2010

Urbana, Illinois

Adviser:

Assistant Professor Lance C. Schideman

ABSTRACT

This study assesses the net energy balance and economic benefits of harvesting detrimental environmental algal blooms and conversion of the harvested biomass into biofuels. An engineering model was developed to compare the energy efficiency of different harvesting methods and biofuel conversion techniques. The modeling data was largely compiled from a variety of literature sources, but was also supplemented by some original experimental data as necessary. The recurring algal blooms that lead to the hypoxic zone in the Northern Gulf of Mexico was used as a case study situation. Three different harvesting techniques: plankton net trawling, traveling screen, and screw pump filtration, were compared in terms of energy consumption and harvesting efficiency. Among the various conditions modeled, the most favorable harvesting condition was produced by a 750 kW fishing boat with a plankton trawling net for harvesting algae biomass at 0.5 m/s harvest speed and harvesting from the surface to 0.5 m depth in the ocean. When harvesting a highly eutrophic area (40 mg-chlorophyll/m^3) under these conditions, we estimate a plankton net trawling operation can collect 100 kg of dry algal biomass with 1 GJ of harvesting energetic consumption.

Four different biofuel conversion processes, hydrothermal liquefaction (HTL), anaerobic digestion (AD), transesterification and fermentation, were compared in the model. Hydrothermal liquefaction and anaerobic digestion are generally more favorable in terms of energy production because they process a larger portion of the algal cell and require less dewatering. The dewatering energy required for transesterification and fermentation leads to a negative energy balance for these processes. Integrated conversion processes of transesterification combined with AD or HTL were also considered, but these combinations still produced negative energy balances. Overall, the energetic analysis revealed that the entire harvesting and conversion process can achieve an energy "break-even point" if the chlorophyll concentration is above 55 mg/m^3.

To evaluate potential improvements in energy efficiency, basic surface harvesting was compared with vertical focusing of algal biomass. Our estimates indicate that basic surface harvesting technology can harvest 1596 metric tons in 3 months and reduce the net cost of $93,357,016. Vertical focusing potentially could increase the harvest to 23,313 metric tons over 3 months and reduce the net cost to for $81,380,937. This analysis showed that vertical focusing

technology can offset 98% of harvesting energy in April. Environmental analysis showed that harvesting natural occurring algae in Atchafalaya and Mississippi delta once a month reduces nitrogen flows into the Gulf of Mexico by 0.5%.

ACKNOWLEDGEMENTS

My heartfelt thanks go to the many people who have helped me throughout this project. Primary thanks go to my advisor, Dr. Lance Schideman, for his guidance, support and patience. He always provides valuable suggestions and clever ideas. He taught me the importance of critical thinking and professional development. His enthusiasm for scientific research in the field of algal biofuel inspired me to be a better researcher. I am fortunately working in his lab.

Also, I would like to thank my other committee members, Dr. Grift and Dr. Rodriguez. Without their help and advices, this project would not have been finished.

I would also like to thank all my coworks, Kyle Hegger, Yan Zhou, Peng Li, Jianping Wang, Derek Vardon, Mai Pham, Joel Krehbiel, Guo Yu, Zhichao Wang and Oliver Hui. I am lucky to have worked with such a supportive and genuine group of people. Especially Kyle, who started the proposal of this project and helped me planning on the steps to finish the project.

I also want to thank all my friends and families, especially my parents, Sung-Lin Kuo and Yueh-Chiu Lin who provided encouragement and support throughout the years. I love you and miss the days living closer to you. Thank you all.

CONTENTS

1. INTRODUCTION

1.1. Justification

1.1.1. Eutrophication in the Gulf of Mexico

Eutrophication is a phenomenon in which pollution of aquatic ecosystems with excessive nutrients like nitrogen and phosphorus results in increased primary productivity by phototrophic bacteria, algae and higher aquatic plants. It is now recognized to be one of the most important factors contributing to habitat change and temporal expansion of harmful algal blooms (HABs) (Anderson, 2002). Sewage discharge and runoff from agriculture have been identified as the main sources of nutrient pollution. Both nitrogen and phosphorus have been implicated as contributing to eutrophication, but nitrogen has received more attention because the amount of nitrogen used in fertilizers is far greater than phosphorus (Dolan et al., 2007). Elevated levels of nutrients can change the phytoplankton community composition through induced changes in predation, resource limitation, light availability and biological effects on sediments (Anderson et al., 2001). Many studies have examined the relationship between HABs and inorganic nutrient ratios, such as N:P or N:Si. In areas with high silica concentrations, *Rhopalodia gibberula* and *Nitzschia palea* were found to be the primary dominant species. Blue-green algae are abundant in marine area with less sewage pollutant (Dortch et al., 2001).

There is significant evidence showing that eutrophication problems in the United States are widespread. In one study of over 100 U.S. estuaries, 40% reportedly suffered high expression of eutrophic conditions, and another 36% had moderately eutrophic conditions (Bricker, 1999). The primary eutrophic symptoms in this survey were decreased light transparency, high chlorophyll a concentration, and change in algal dominance. The composition of phytoplankton depends on a balance of many factors, and phytoplankton ecology needs to be viewed within the context of spatial heterogeneity and seasonal variations (Platon et al., 2005). There are approximately 5000 marine phytoplankton species, and 300 species are known to occur at high enough concentration to discolor seawater. Forty to fifty of these species have the ability to produce toxins that are harmful to marine creatures or humans. Damages from a single event of *Karenia brevis* in North Carolina, USA, in 1987-88 were estimated at over $30 million, and the average annual losses in the US have been conservatively estimated to be over $50 million (Anderson et al., 2000). In 1998, the value of farmed Atlantic salmon and rainbow trout in Norway was approximately

US$1 billion, with an estimated loss of US$2 million per year attributed to HABs. Effective monitoring and remedial action can reduce that loss (Stumpf and Tomlinson, 2005).

1.1.2. Hypoxia in the Gulf of Mexico

Hypoxia describes a condition of low dissolved oxygen content (< 2mg/L) in natural water bodies that is environmentally undesirable because it does not support most marine creatures and can result in large-scale kills of aquatic animals. Hypoxia typically occurs following a large-scale algae bloom that dies off and is subsequently consumed by heterotrophic bacteria, which deplete all the available oxygen in the water column. Major coastal hypoxic zones are known to occur in approximately 146 locations around the globe and can cover vast oceanic expanses, larger than 90,000 km^2 in some cases (Joyce, 2000; Dybas, 2005). The largest recurring hypoxic zone in the coastal waters of North America is located along the continental shelf of Louisiana and Texas adjacent to the mouth of the Mississippi and Atchafalaya River Basin (MARB). This river basin drains approximately 40% of the contiguous United States and delivers runoff with elevated nutrient levels from America's agricultural heartland to the Gulf of Mexico (EPA, 2007). Although hypoxia in the Gulf of Mexico may not be an exclusively modern phenomenon, the size and duration of historical algae blooms before 1940 were small in comparison to recent ones. Since the mid 20th century, when heavy fertilization became a widespread practice in modern agricultural practices and significant changes in flow patterns through the MARB delta have occurred, the Gulf has seen a substantial growth in the average size and severity of its hypoxic zone, which has swelled to more than 20,000 km^2 in some recent years (Rabalais et al., 2001). The historical trends have shown significant increases in gulf algae production since the 1950s (CENR, 2000).

Problems with hypoxic zones stem from the fact that higher species of marine life will either retreat or die, which can litter the ocean with marine animal corpses. Hypoxia effectively reduces the available marine habitat, which is a significant concern because the Gulf of Mexico supports over 40% of the nation's commercial fishing with typical annual yields of more than a billion pounds of fish with a total market value of around $700 million (NOAA, 2008). Dwindling fish stocks and increased travel distances to access fertile water has resulted in decreasing fuel efficiency across the global fishing industry, which consumes approximately 50 billion liters of fuel per year (Tyedmers et al., 2005). In addition, low oxygen levels in the Gulf create a benthic

layer on the ocean bottom that is dominated by metal or sulfur reduction bacteria, which contribute to stark color and odor difference in the hypoxic zones (Eldridge and Morse, 2008). The resulting smell and discoloration is objectionable and can have detrimental effects on recreational activities and tourism (Rabalais et al., 1999)

1.1.3. Current Hypoxia Mitigation Proposals

Many researchers have concluded that nutrient loads significantly contribute to hypoxia and have determined that Gulf algae are naturally nitrogen limited until the seasonal influx of riverine nitrogen at which time phosphorous becomes limiting (Sylvan et al., 2006).Therefore, the EPA hypoxia science advisory board has suggested an initial target to reduce fertilizer usage by 40%-45% (EPA, 2007). This measure effectively addresses the root cause of the hypoxia, but it also has potential drawbacks such as an increased risk of reduced crop yields. Additionally, mandated fertilizer reductions could be difficult to implement due to resistance from the agricultural industry and difficulties in establishing appropriate baseline conditions given the natural variation in fertilizer applications based on crop selection, seed characteristics, soil and even meteorological conditions. Finally, this approach has a significant time delay before environmental benefits are fully realized. Some researchers have claimed that even if all fertilizer usage is halted, the size of the hypoxic zone will gradually shrink over years because of the nutrients stored in the sediment will refertilize the water column (Turner et al., 2008). Another proposed mitigation alternative is to convert 5 million acres of riparian farmlands to wetlands, which would filter out nutrients before they flow into the Gulf. However this alternative has been estimated to cost about $4.9 billion, including the annual value of displaced crops (CENR, 1999). In addition, converting riparian farmlands into wetland still suffer of lag periods. Therefore, developing hypoxia mitigation alternatives that avoid this lag period are needed and would complement the proposed long-term reductions in fertilizer usage.

A new approach for mitigating hypoxia is proposed in this study, which is to harvest algal blooms prior to the onset of their death phase. One important advantage of this alternative is a fast response time with the immediate realization of environmental benefits. Harvesting algae from a water body immediately decreases the organic content of the water, thus limiting the heterotrophic bacteria growth that leads to hypoxic conditions. The other major advantage is that we can convert harvested algae into valuable products like biofuel or extract special proteins,

which can offset the cost for harvesting algae from a hypoxic zone (Sheehan et al., 1998; Akkerman et al., 2002).

1.1.4. Biofuel Development

Intensive use of fossil fuels contributes to increasing concentrations of carbon dioxide in the atmosphere, which has been broadly implicated as a cause of global climate change. The 2009 United Nation's Climate Change Conference in Copenhagen asked member countries to take action toward greenhouse gas reduction. After this summit, U.S. President Barack Obama ordered the federal government to reduce greenhouse gas emissions 28% by 2020. The Environmental Protection Agency (EPA) has set a goal for production of 36 billion gallons of biofuel by 2022 to achieve energy independence and CO_2 emission reduction (Mc Carl and Boadu, 2009). It has been reported by the Intergovernmental Panel on Climate Change (IPCC) that biofuel is an essential strategy for mitigating global warming (Parry et al., 2007).

Biofuel feedstock can be described by three main generations. The first generation biofuel feedstock is food or oil crops like corn, rapeseed, and soy (Patil et al., 2008). Biofuel produced from first generation feedstock has attained commercial scale use with government subsidy for each gallon produced. It is predicted that both production and consumption of biofuels will continue to increase in the foreseeable future. However, it is difficult to meet the transportation fuel demand with these crops because of the following factors:

1. Competition for the use of arable land. Producing biofuel from food crops might decrease food production and raise food price.

2. Low areal productivity. Currently, biofuel production uses about 1% of the world's arable land area and supports approximately 1% of the global transportation demand. It is impractical to provide 100% transportation fuel by use all arable land(IEA, 2007).

3. High water and fertilizer requirements could lead to significant resource shortage and would generally increase the cost of biofuels.

Second generation biofuel feedstock include dedicated energy crops like switchgrass, miscanthus and willow (Uellendahl et al., 2008). These crops typically consume less energy to plant and require less nutrient and pesticide application. Additionally, perennial crops have a

longer growing season, and thus can have higher annual solar energy conversion efficiency. In addition, it is a better habitat for more diverse wildlife (DOE, 2006). However, these feedstock consist of lignocelluloses structures and pretreatment is needed to breakdown this material into sugars for downstream biofuel conversion.

Algae belong to the third generation of biofuel feedstock and are a promising source of biomass and can produce a variety of desirable oily products (Chisti, 2008). Compared to other terrestrial biofuel crops, algae have much higher biomass production per unit area. Algal biomass productivity is much higher than other proposed biofuel crops. Secondly, unlike corn for ethanol, algae are not a major food crop, and thus developing algae biofuel further reduces the competition between with food and fuel. Third, while algae grow photosynthetically, they sequester CO_2 and uptake essential nutrients from water, which provides opportunities to combine algal culture systems with wastewater treatment or power plant emission control systems (Clarens et al., 2010).

1.1.5. Algae Cultivation Technologies

Current algal culturing technology can be divided into two main categories: open culture systems and closed photobioreactor (PBR) systems. Open culture systems usually grow algae in an open environment such as lake or pond. Thus, the cost of building an open-pond system is less expensive than PBR system. However, open pond systems are generally lower in productivity due to less control over temperature, light, evaporation, and contamination by wild species, which can significantly decrease biomass productivity. Moreover, there is only 300–600 ppm CO_2 in the atmosphere, which could suppress algal growth rates because of low carbon source available (Mata et al., 2010).

PBR is a closed system that reduces contamination concerns and allows for optimization of reactor conditions to support various algae species' biological and physiological characteristics. Most PBR systems are unique designs, built to meet specific production goals. Generally, PBRs have the following features that differentiate them from open pond systems:

1. PBRs provide for good control of important reactor conditions like temperature, light, CO2, mixing, pH and others. Therefore, the productivity of a PBR is usually 3-5 times higher than an open pond system (Brennan and Owende, 2010).

2. Closed systems prevent water evaporation and therefore reduce water consumption.

3. High density cultivation results in less energy consumption during harvesting and dewatering. However, there are some drawbacks that should be considered while using PBR: First, most PBRs use sunlight as the light source, which means productivity will be strongly related to weather. Also, biofilms can build up in the reactor, therefore a routine air scour or cleaning is needed.

4. Excess photons become heat stored in the reactor, and thus cooling process need to be considered.

5. High construction and operational costs. The cost of biomass production from PBR might be one order of magnitude higher than biomass production in open pond system (Schenk et al., 2008).

1.2. Objectives

Based on the previous justification, eutrophication and hypoxia are environmentally undesirable phenomenon that have an increasingly large impact on coastal economics and public health. Even now, there exists no effective mitigation process that could solve this situation. On the other hand, although algae biofuel has a lot of potential in terms of oil productivity and CO_2 sequestration, the huge production cost remains a problem. Therefore, in this study we have established the following objectives:

1. Propose a new concept for mitigating hypoxic zone. The basic harvesting technique will be modeled from that of existing algae collection operations, where floating vessels will drive through the bloom to collect floating algae that can be processed on the collection vessel or later on shore where it will be converted to biocrude oil. Harvesting algae for biofuel production offsets the harvest costs and energy usage for harvesting algae by converting harvested algae to biofuel.

2. Development of an engineering-economic model. Evaluate the range of expected conditions to determine the favorability of cost and energy balances. Estimate the system impacts of different collection strategies and different end product processing schemes to identify the most promising paths for research and practical applications.

3. Investigate and evaluate opportunities for further research. This study will identify the most important parameters that can significantly improve the cost and benefits of harvesting algae from natural waterbodies. We will use these parameters to guide future designs of algae harvesting equipment.

In the end of this research, we will present the economic and energy balances for the current state of the art, and highlight promising alternatives for future technological development. This analysis will lead to a strategic roadmap for developing algae harvesting techniques as a cost-effective alternative for addressing hypoxia problems.

2. MODEL DEVELOPMENT

2.1. Harvested Algae Biofuel Energy Recovery Model

To understand the effects of harvesting environmental algal blooms and converting the biomass into biofuels, we evaluated the overall energy balance of the entire process for a variety of different harvesting methods, conversion processes and end products. An engineering process model was developed and implemented in a Microsoft Excel spreadsheet to collect information from a large number of literature sources, calculate the energy balances, and investigate the sensitivity of the energy balance to variations in input parameters. This model is named the Harvested Algae Biofuel Energy Recovery model (HABER) and includes a set of Excel worksheets including input parameters like algae characteristics, harvesting processes, refinery methods and end product values. Input parameter values and ranges have been identified from scientific literature and industrial experience, which draws from a variety of disciplines related to the proposed hypoxia mitigation strategy. For example, energy for plankton net trawling was taken from the fishing industry, and information on biodiesel conversion of different algae species was provided by published literature in the biofuels area. This model allows manipulation of specific parameters and determines the resulting effects on the whole energy balance, which was used to identify the most promising factors for improving the whole system.

Figure 2-1 provides an overview of the major components of the HABER model and the primary input parameters. For each of these parameters, the following section tables provide symbols, units, default values, and parameter ranges available from the scientific literature. Figure 2-2 shows the interface of HABER model.

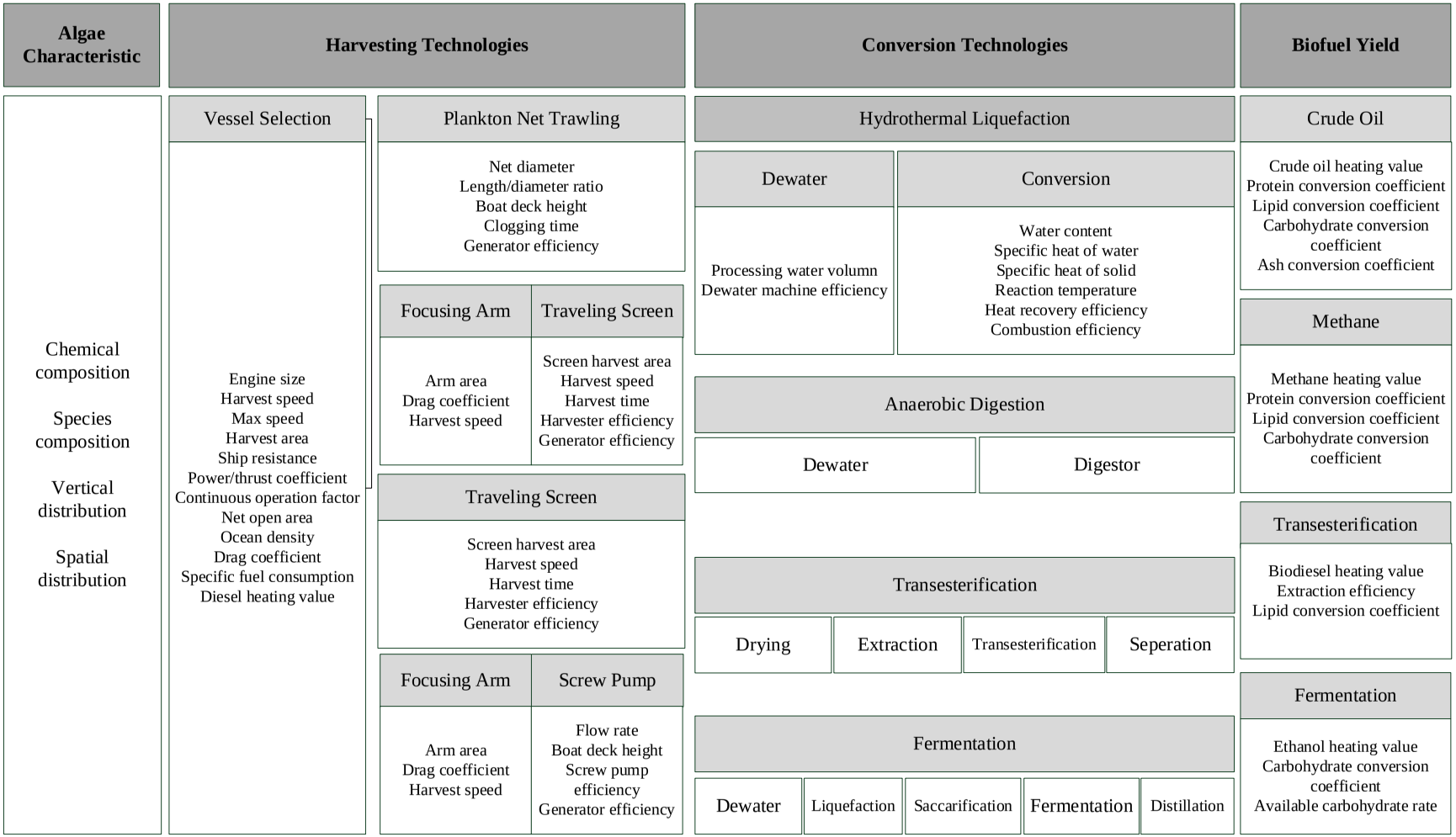

Figure 2-1. Process scheme of HABER model.

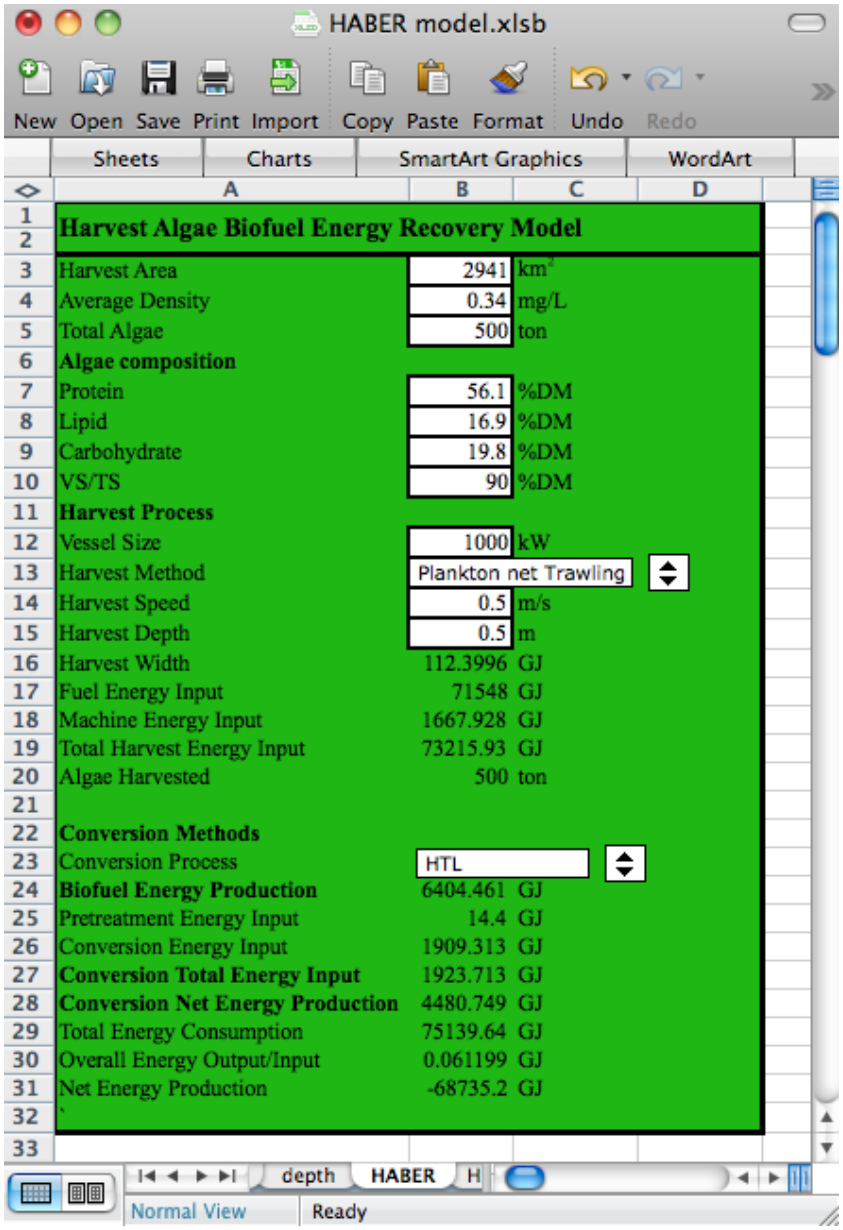

Figure 2-2. HABER model interface.

2.2. Algae Characteristics

In the HABER model, algae characteristics are major input parameters, which determine the total available algae biomass in a bloom event and algae chemical composition. The following section describes the dominant species in the Gulf, species chemical compositions, and methods used for estimating the primary production of algae in the Gulf of Mexico.

2.2.1. Gulf of Mexico Algal Biomass

The work of this study was focused on the northern Gulf of Mexico (88°00W-92°00W, 28°00N- 31°00N). The area covers the most severe hypoxic area and the Mississippi river estuary. In this model, we use satellite-based chlorophyll data provided by Louisiana State University Earth Scan Laboratory, to estimate ocean productivity. The data was collected from Seastar Satellite, which was launched with a Sea Viewing Wide Field-of-View Sensor (sea-WiFS). The ocean color sensor measures radiance from two components, a water-leaving component and an atmospheric component. Water-leaving radiance is determined by the ratio of backscatter to absorption summed for the upper portion of the water column. The water characteristic color signatures can be derived from the wavelength-dependent backscatter and absorption. For example, clear water appears blue as it absorbs red light (600-700 nm) and reflects blue light (400-500nm). During an algae bloom, chlorophyll absorbs red and blue light and reflects green light (500-600nm) (McClain, 2009). Therefore, algal blooms can be characterized as green in color. One key feature of satellite imaging is that the sampling depth, also called visibility depth, can vary. It may range from 20 meters in clear water to as little as 1-2 meters in high chlorophyll concentration areas (MacFadyen, 1999). Remote sensing technologies allow for more complete coverage of the study area than ship-based measurements. They provide temporal and spatial data that represent the overall condition within the study area.

The raw data collected from Earth Scan Laboratory are JPEG picture files. These data are the highest resolution satellite images, and measured chlorophyll data available and are at a resolution of 360 m^2. To estimate the total chlorophyll concentration in the field and identify high chlorophyll density areas, a MATLAB® program was developed for image processing.

Figure 2-3 shows the main steps of image processing. Graph A is the raw satellite image of chlorophyll concentration. The first step is locating the study site, which is in the upper left corner of graph A with the coordinates 88°00W-92°00W, 28°00N- 31°00N, which is shown in graph B. The next step is creating a boundary filter to screen out the land area. Next, the sum of chlorophyll and average chlorophyll can be calculated in graph C. The final step is creating different level of chlorophyll concentration filter to screen out chlorophyll densities that are below a certain threshold.

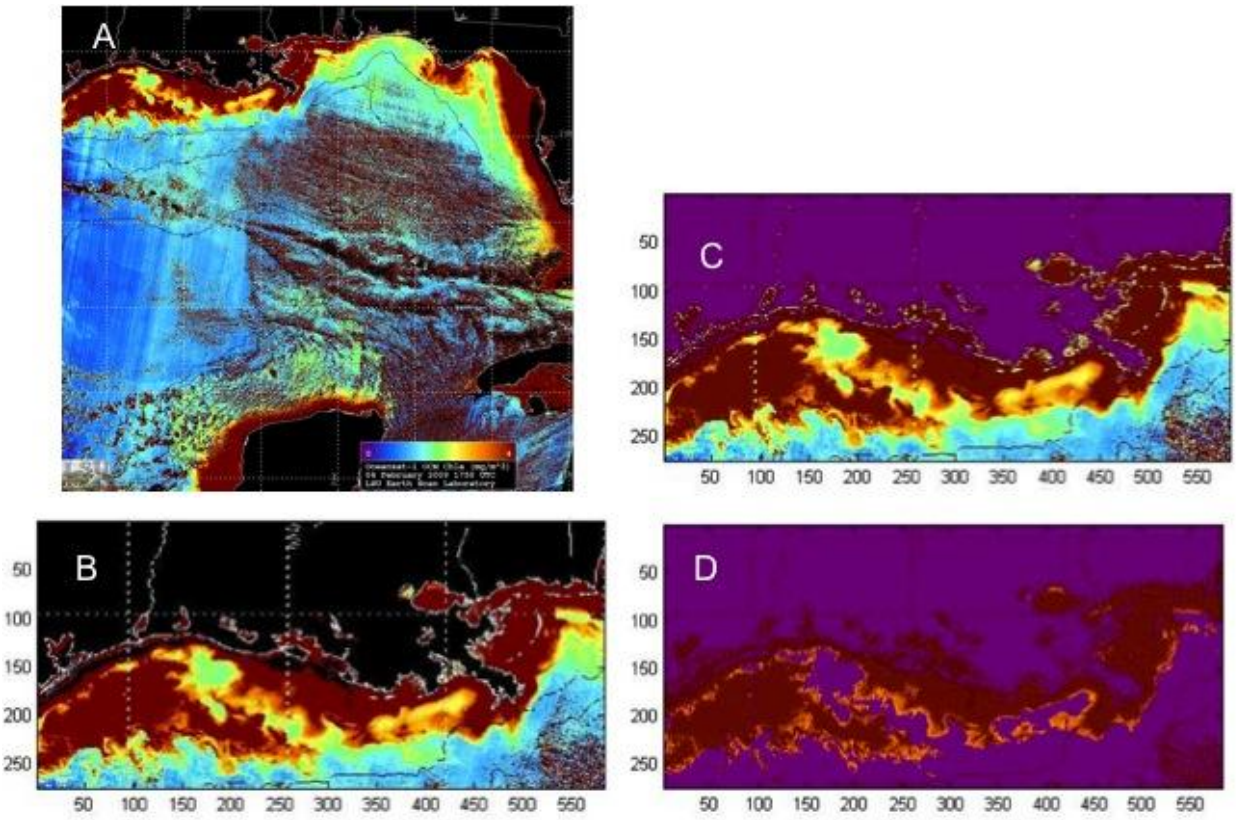

Figure 2-3. SeaWiFS image proceed by MATLAB®, (A) shows the raw image obtained from Louisiana State University, (B) shows the location of study site (88°00W-92°00W, 28°00N-31°00N), (C) shows the image after filtered land area, (D) shows the image after filtered low chlorophyll density area.

Past research has developed a quadratic model to describe the relationship between the radiance value and in-situ measurements of chlorophyll density in the northern Gulf of Mexico (Walker and Rabalais, 2006). The relationship is shown below

$$Y = 1.4013X - 0.0222X^2 \quad (1)$$

Where Y is the in-situ measurement value of chlorophyll density (mg/m^3), and X is the satellite received chlorophyll concentration value, in mg/m^3 (Walker and Rabalais, 2006). This regression had an r^2 value of 0.89. However, the chlorophyll concentration measured from satellite image is the average concentration of whole water column from surface to visibility depth. To estimate the whole biomass in water column, the visibility depth is an essential parameter.

2.2.2. Vertical Distribution Model

Algal communities are not always floating at the surface. Algae require both light and nutrients to grow phototrophically, and therefore position themselves in the water column to find conditions where both light and nutrient concentrations are sufficient (Sutor, 2007). However, in the ocean the light sufficient zones and nutrient sufficient zones are not necessarily co-located.

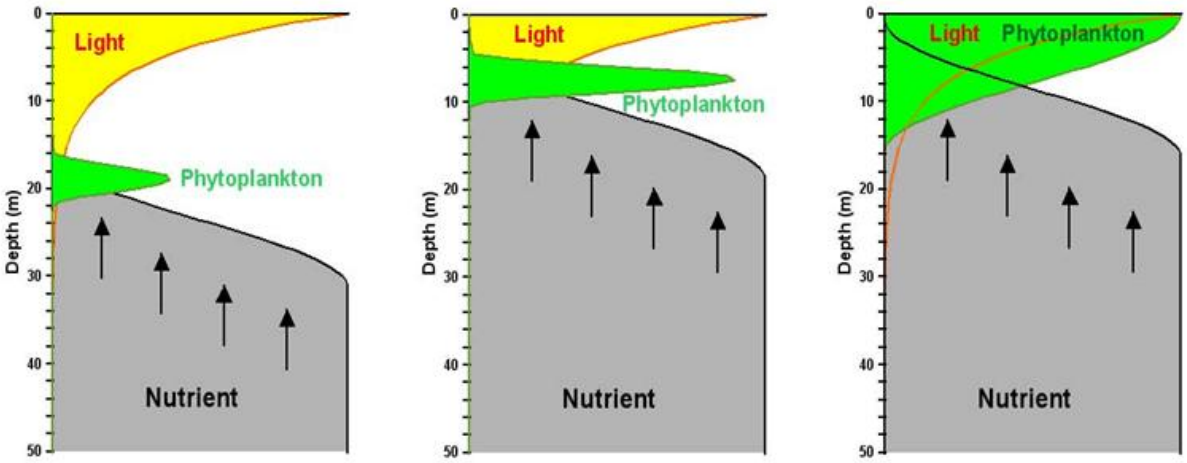

Figure 2-4. Light zone and nutrient zone effect on algal vertical distribution **(**Nezlin, 2009).

As shown in Figure 2-4, algae grow best at a depth where favorable light and nutrient conditions intersect. Therefore, at the location near the coast or estuary where there is strong mixing throughout the whole water column, the algae usually have highest density at the ocean surface. To account for the vertical distribution, we assumed that algae are present at the highest density near the surface during an algae bloom (Kuster, 2008). The optical depth of the mixed layer in nutrient-rich system is between 5 to 10 meters (Wofsy, 1983). Therefore, we create a linear vertical distribution model assuming the highest algal density is at ocean surface and the visibility depth is 5 meters. The simulated distribution is shown as Figure 2-5.

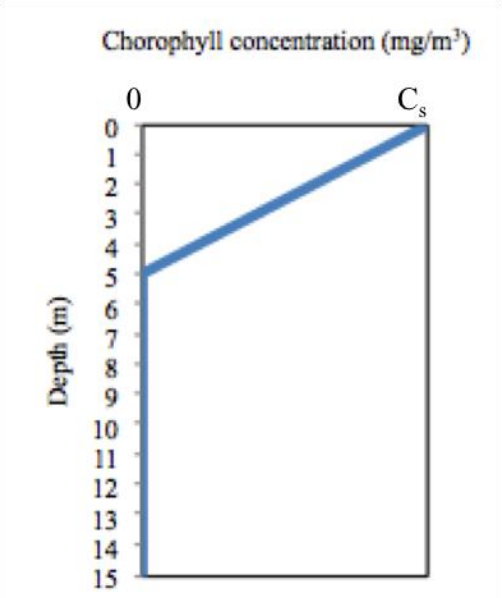

Figure 2-5. Vertical density distribution simulation model.

Based on this vertical distribution model, the relationship between satellite measured chlorophyll concentration and surface chlorophyll concentration can be described as Equation (2)

$$C_s = 2C_{average} \tag{2}$$

Where C_s is the surface chlorophyll concentration, in mg/m^3. $C_{average}$ is satellite measured average chlorophyll concentration in water column, in mg/m^3. Therefore, the total amount of chlorophyll harvested from the surface to D depth in a given area can be expressed as Equation (3)

$$M = \int_{u=0}^{u=D} \left(\frac{C_s}{D_m} u + C_s\right) du \tag{3}$$

Where M is the total chlorophyll concentration from surface to D meters depth in unit area, mg/m^2. D is harvest depth in meters, C_s is the surface chlorophyll concentration, mg/m^3, D_m is the visibility depth, assumed 5 meters.

2.2.3. Dominant Algal Species in the Gulf of Mexico

In the Gulf of Mexico, diatoms are the dominant biomass communities of many marine and estuarine areas, particularly in spring (Walker and Rabalais, 2006). Diatoms require silicon to build their cell walls. If silica is limited, other non-siliceous species proliferate, such as dinoflagellates or cyanobacteria, which will replace diatoms and become dominant species.

Diatoms, cyanobacteria and dinoflagellates are the most important proportion of phytoplankton communities. In the HABER model, literature on the typical chlorophyll percentage of different algal species was used to calculate the total biomass from chlorophyll density. Additionally, literature on typical macromolecule compositions of algae was used for biofuel conversion estimates. In particular, four major components: protein, carbohydrate, lipid and ash, were used to estimate biofuel production from different algae species. Finally, the typical size of different algal species as reported in the literature also provides essential information for harvesting analysis.

Skeletonema costatum, Chaetoceros calcitrans, Thalassionema nitzschioides Rhizosolenium sp. are the major organisms present in diatom communities of the Gulf of Mexico (Walker and Rabalais, 2006). The size of these diatoms are usually above 20 μm, therefore they are much easier to harvest comparing to picocyanobacteria. *Karenia brevis* is identified as a harmful algae that produces algal toxin. The size of *Karenia brevis* is between 18 and 45 μm, which is also easy to collect. Picoplankton is an example of algae that are very small (<2 μm), and they can only be harvested by a very fine mesh or after auto-aggregation. The species biochemical composition is shown in Table 2-1.

The relationship between chlorophyll concentration and algal biomass varies due to the seasonal changes in the dominant species. Our approach of estimating algal biomass was using the long-term monthly species community data in the gulf, and combining with species chlorophyll concentration to calculate monthly algal biomass/chlorophyll ratio. We then convert total chlorophyll concentration in the gulf into total algal biomass.

Table 2-1. Common algal species biochemical composition.

Species	Chlorophy a (%)	Protein (%)	Carbohydrate (%)	Lipid (%)	Ash (%)	Size(μm)
Diatom average	1.5	30	18.0	20		
Skeletonema costatum[a]	1.8	37	20.8	6.9	39	30
Chaetoceros calcitrans[a]	1.5	34	6.0	16	28	80
Thalassionema nitzschioides[a]	0.95	34	8.8	19		10~110
Rhizosolenium sp[b]		36	28.7	34.8		6~9
Picoplankton Average	1~3	56.1	19.8	16.9	7.2	<2
Synechococcus[c]		63	15.0	5		
Chlorophyceae Nannochloris[d]	1.6	30	23.0	21	26	2
Dinoflagellate						
Karenia brevis[e]	5.8	20.9	46.5	11.6	15.11	18~45
Phytoplankton		20.8	22.3	45.7	11.2	2~20

a. Hasle et al., 1996
b. CIMT, 2010
c. Sevilla, 2006
d. Algaefuel, 2010
e. Orlando Sentinel, 2009

Figure 2-6 reveals five years average (1990-1995) algal species community data at a fixed station in the Gulf of Mexico (Dortch et al., 2001). The abundance of diatoms and other algal species are indicated by left vertical axis, the abundance of picocyanobacteria shows in right vertical axis. Diatoms are present in February, March April, May and December. Note that there are no data presented in January, assuming it is the same as February. Therefore, diatoms and other phytoplankton are estimated to be 40% of the amount in January and February. Picocyanobacteria are the dominant species for most of the time, from May to November. Combining Table 2-1 and Figure 2-6, estimated monthly biomass chemical composition is generated to serve as model database. The harvested biomass chemical composition simulation at different month is shown in Table 2-2.

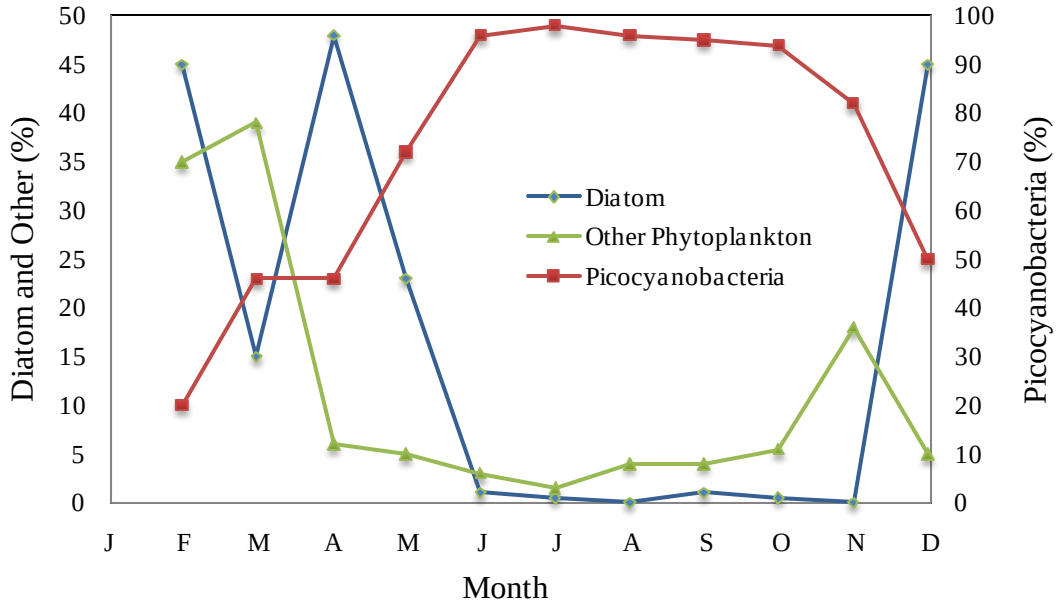

Figure 2-6. Dominant communities in the Gulf of Mexico from 1990-1995 (Dortch et al., 2001). The abundance of diatoms and other algal species are indicated by left vertical axis, the abundance of picocyanobacteria shows in right vertical axis.

Table 2-2. Simulated monthly biomass biochemical composition.

Month	Diatom[a] (%)	Picoplankton[a] (%)	Others[a] (%)	Chlorophyll[b] (%)	Protein[b] (%)	Carbohydrate[b] (%)	Lipid[b] (%)	Ash[b] (%)
January	40	20	40	2.82	31.58	29.76	16.02	20.28
February	45	15	40	2.77	30.28	29.67	16.18	21.52
March	20	50	30	1.35	52.19	19.53	17.37	10.92
April	45	50	5	1.05	44.36	18.99	18.30	18.36
May	25	75	0	1.25	49.58	19.35	17.68	13.4
June	0	100	0	1.5	56.10	19.8	16.90	7.20
July	0	100	0	1.5	56.10	19.8	16.90	7.20
August	0	100	0	1.5	56.10	19.8	16.90	7.20
September	0	100	0	1.5	56.10	19.8	16.90	7.20
October	0	100	0	1.5	56.10	19.8	16.90	7.20
November	0	85	15	2.145	50.82	23.805	16.11	8.39
December	45	55	0	1.05	44.36	18.99	18.30	18.36

a. Percents of algal communities in the Gulf of Mexico
b. Percents of dry algal biomass

2.3. Harvesting Energy Consumption Model

To estimate the energy input of different harvesting scenarios and to determine the most advantageous conditions for key parameters, a sub-model called the Harvesting Energy Consumption Model (HECM) was constructed. As shown in Figure 2-7, there are five key components in the model. They are harvest vessel, focusing arm, plankton net trawling, traveling screen and screw pump. In the model, first we evaluated vessel engine size and harvest speed. Then we evaluated four potential harvesting methods:

1. Harvest algae by a trawling plankton net.
2. Install focusing arms on the both side of the boat with certain angle, when harvest vessel moving forward, the focusing arm will lead the floating particles toward the ship and collected by the traveling screen.
3. Use only a traveling screen to harvest floating algae.
4. Centralize algae by focusing arms and harvest by a screw pump and screening system.

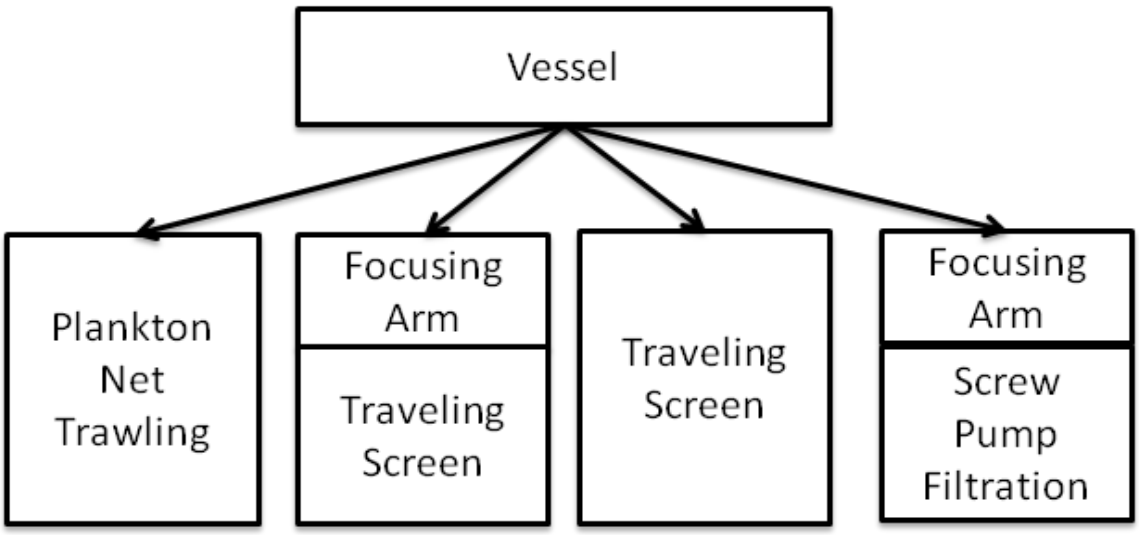

Figure 2-7. Harvesting energy consumption model scheme.

2.3.1. Vessel

In this study, we assumed that existing marine vessels would be outfitted with harvesting equipment for gathering algal biomass. There are two major categories of marine vessels distinguished by traveling distance: ocean-going and non-oceangoing vessel (Bentz, 1997). Booz (1991) categorizes oceangoing vessels into four types: 1. container ships; 2. tankers and bulk carriers; 3. General cargo carriers and oceangoing tugs; 4. Passenger liners and cruise ships. In the same report, Booz-Allen simply classified non-oceangoing vessels by type and power. They are: 1. Fishing vessels; 2. Tugs; 3. Passenger ferries; 4. Dredging and construction ships 5. Work/crew boats (Booz, 1991). A fishing vessel was selected because it is the most common vessel and has a large range of sizes and engine power available. The engine power determines two major harvesting parameters: cruise speed and harvest width. These two parameters are negatively correlated to each other. When the boat increases harvesting cruise speed, the ship receives more resistance from the harvesting equipment, and ultimately there is a maximum speed that balances the harvesting equipment resistance and the boats forward thrust.

Fishing vessels use 85% of total power for operations like dragging a net (Prado, 1990). This effective power is used to estimate the maximum harvest width at different speeds and different engine power. The time needed for harvesting a unit area can be calculated by dividing area to harvest width and harvest speed. Therefore, total fuel consumption for harvesting unit area can be obtained by the time consumed and fuel consumption rate of specific vessels.

2.3.2. Focusing Arm

The aim of the focusing is to provide mechanical barriers that are capable of centralizing the wide spread floating algae while the harvesting vessel is moving forward. Therefore it condenses algal cell density and reduces the size of harvesting machine. In the HABER model, we provide the option of combining basic harvesting method with or without focusing arms.

A focusing arm is assumed to be made by a floating boom. Floating booms are commonly method that used to confine floating substance like spilled oil, debris or brine shrimp cysts (Lamon, 1996). There are various types of floating boom: 1. Curtain booms: often used in offshore situations with good wave response. 2. Fence booms: used in high-current areas. 3. Shore sealing booms: used as a barrier 4. Fire-resistant booms: used in conjunction with in-situ burning techniques (Ventikos et al., 2004). Figure 2-8 shows a pilot test of an open ocean oil

skimmer combined with floating booms, design by Omsett, Inc. The experiments showed that floating booms can effectively focus floating oil by using waves and current.

Gröndahl (2009) had conducted a pilot project that modified floating booms for Baltic Sea surface cyanobacteria bloom removal. He modified the subsurface skirt into a forming fabric for successfully focusing and removing cyanobacteria from water.

Figure 2-8. Pilot test of the "Big Crew" oil skimmer with floating boom (Omsett, 2010).

2.3.3. Plankton Net Trawling

A plankton net is a device that can be used to collect little plants and animals that live in the ocean or freshwater. It is usually a funnel-shaped, fine-meshed net that is towed through the water, shown as Figure 2-9. A plankton net concentrates plankton from hundreds of gallons of water that pass through it. Ring nets are the simplest design of plankton nets. They are towed using a key ring and three strands which are tied onto a wire hoop. The hoop itself holds a cylinder of fine mesh net. The bottom of the plankton net is bound to a plastic bottle. When the net is pulled through seawater, larger particles do not pass through the net and will be trapped and collected within the bottle. The net is usually deployed vertically for non-quantitative purposes from a platform, such as a vessel or pier. It may also be towed, although it lacks in devices for controlling its passage through the water column, which is otherwise determined by

hydrodynamic forces generated naturally during towing or hauling. Towing applications are mainly non-quantitative. When a rectangular frame of 1 × 0.6 m and a mesh of 160 µm are installed on a fishing boat and moved at a speed of 1.5 km/h average yields of 40 kg live zooplankton can be harvested in 1 h. To minimize the damage to the concentrated plankton, the nets must be emptied every 15 to 30 min (Lavens and Sorgeloos, 1996).

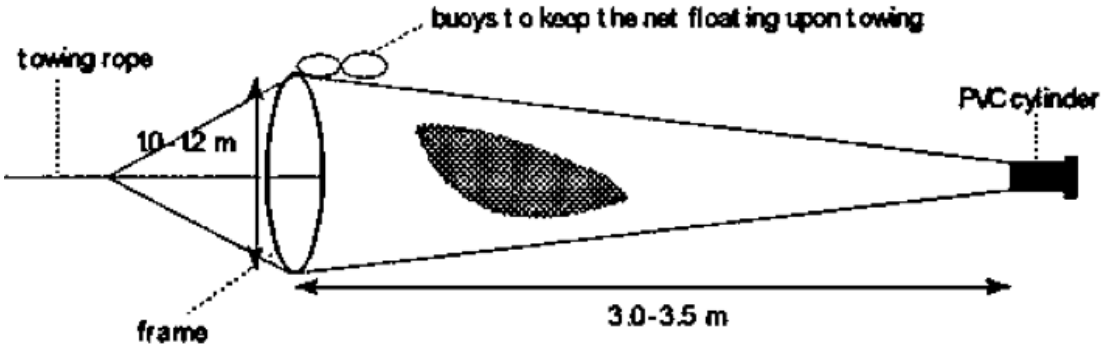

Figure 2-9. Plankton net scheme (Lavens and Sorgeloos, 1996).

In some cases, scientists have coupled two plankton nets together to have a broader collection area. This is called a bongo net, shown as Figure 2-10. The name is due to the perceived resemblance to the paired drums. The mesh size is very fine, ranging from 20 µm up to 1000 µm. The nets, mounted on a rigid yoke, can be towed from the surface to near the bottom for sampling throughout the water column. Most bongo and ring nets are deployed with mechanical or electronic flow meters positioned in the mouth of the net to quantify the volume of water filtered.

Figure 2-10. A set of bongo nets is hauled in and inspected by National Oceanic and Atomospheric Adminstration (NOAA) Ship McArthur crew members (NOAA, 2007).

2.3.4. Traveling Screen

Screen separation is commonly used for solid-liquid separation. There are various types of screen separators: stationary inclined screens, vibrating screens, in-channel screens and others. Stationary inclined screens use gravity to separate liquid from solids. The solution is pumped to the top of a screen. Liquid will pass through the screen, while solid slides down the screen and be deposited on a collection pad. This type of screen separator is widely used to remove water from manure (Møller et al., 2000). However, it frequently needs washing to keep the screen from cogging. A vibrating screen separator is another type of screen separator. This design has a screen that vibrates rapidly, which helps to keep screen from excessive clogging (Grobbelaar, 2000). Liquid is pumped onto the screen at a controlled rate. The liquid passed through the screen and collected by a container under the screen. Separated solids are collected at the edge of the vibrating screen. Another type of screen called an in-channel flight conveyor screen. This separator consists an inclined screen and series of horizontal bars. The separator can be placed directly into an open wastewater channel, which eliminates the need for sump pump or lift pump. United Marine International LLC. has developed a marine harvest vessel, Trashcat system, with the same concept as the in-channel conveyor screen , shown as Figure 2-11 (UMI, 2010). The Trashcat system has a continuous conveyor mounted on the front of the vessel and has the ability to skim debris or seaweeds as wide as 16 feet (UMI, 2010).

Figure 2-11. Open water algae harvester (UMI, 2010).

However, these separators or conveyors are not designed for harvesting algae. The mesh size of the screen should be adjusted to the micron level for collecting algae cells. But using a small

mesh size screen raises problems. For example, liquid cannot easily pass through the screen, thus the separation rate decreases. Smaller mesh screens are also more easily clogged.

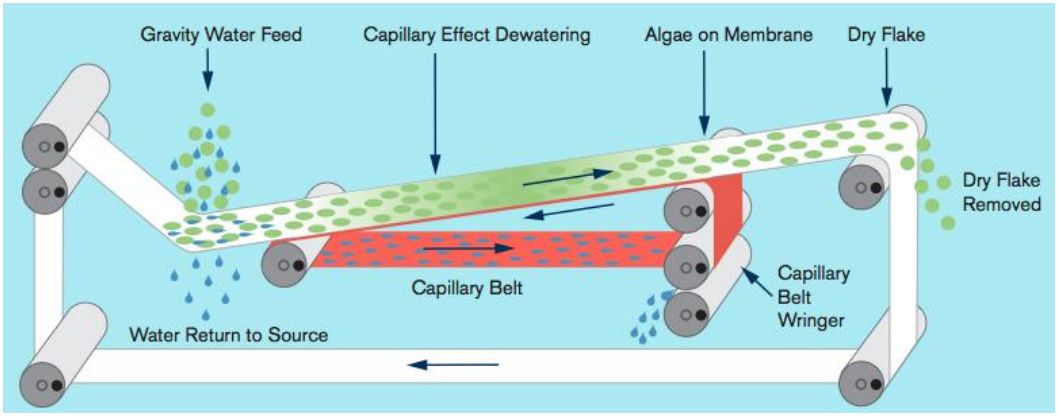

Figure 2-12. AVS-HDD system (AVS, 2010).

AlgaeVenture System (AVS) has developed a Harvesting, Dewatering, and Drying Technology (HDD) to solve this problem, Figure 2-12. The system has synthetic material called superabsorbent polymer fabrics. This material serves as a cap belt that is putted into contact with the bottom of the screen. Because of the molecular bonds from water to water are stronger than water to algae, it can move vast amounts of water and keep algae on the belt. This process allows the system to continuously harvest algae as a thin dry layer. Also, this system uses very little energy since it removes water by absorbance. Base on their prototype, AVS claims the system can process 500 liter of water per hour on less than 40 watts. Therefore, the AVSHDD system provides a great system to mount on marine vessels for algal bloom harvesting.

2.3.5. Screw Pump

A screw pump uses a cylindrical screen with a screw type conveyor in the center. The screw conveys the solids retained on the screen up to the collection end, shown as Figure 2-13 (Møller et al., 2002; White, 1980). Then liquids pass through the screen during transport. A screw pump has a number of advantages over other type of rotor pumps. For example, they are very efficient; screw pump can operate about 70% efficiency for 2/3 of its operating capacity (Burenin, 2002). There is less head required with a screw pump because there are no friction losses by pipes and fittings. Additionally, it is a non-clog configuration thus requiring less operator attention and maintenance. Screw pump have various applications. By adjusting the filter screen pore size, the

screw pump can be used for solids dewatering or water lifting. The separated algal biomass is referred to as cake, but typically still contains 85 to 95 percent moisture (Møller et al., 2002).

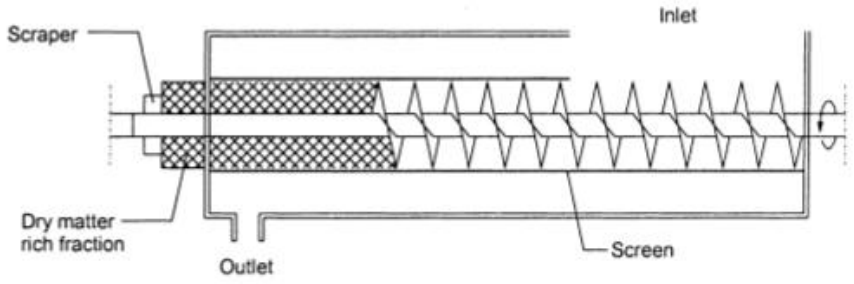

Figure 2-13. Screw pump screen scheme (Møller et al., 2002).

2.4. Harvesting Energy Consumption Model Calculation

The HECM is presented in an EXCEL spreadsheet. The interface of the HECM is showed in Figure 2-14. Four harvesting scenarios are built into the model. Assuming the vessel engine is always fully loaded. All engine power is used against the resistance from ship, machine and focusing arm while moving. Harvesting area is maximized to keep the engine operating at full load. While given a fixed harvest depth, the harvest width extended when harvesting area is increased along with higher engine size. Since the resistance has negative correlation with cruise speed, slower vessel harvesting speed means wider harvesting area.

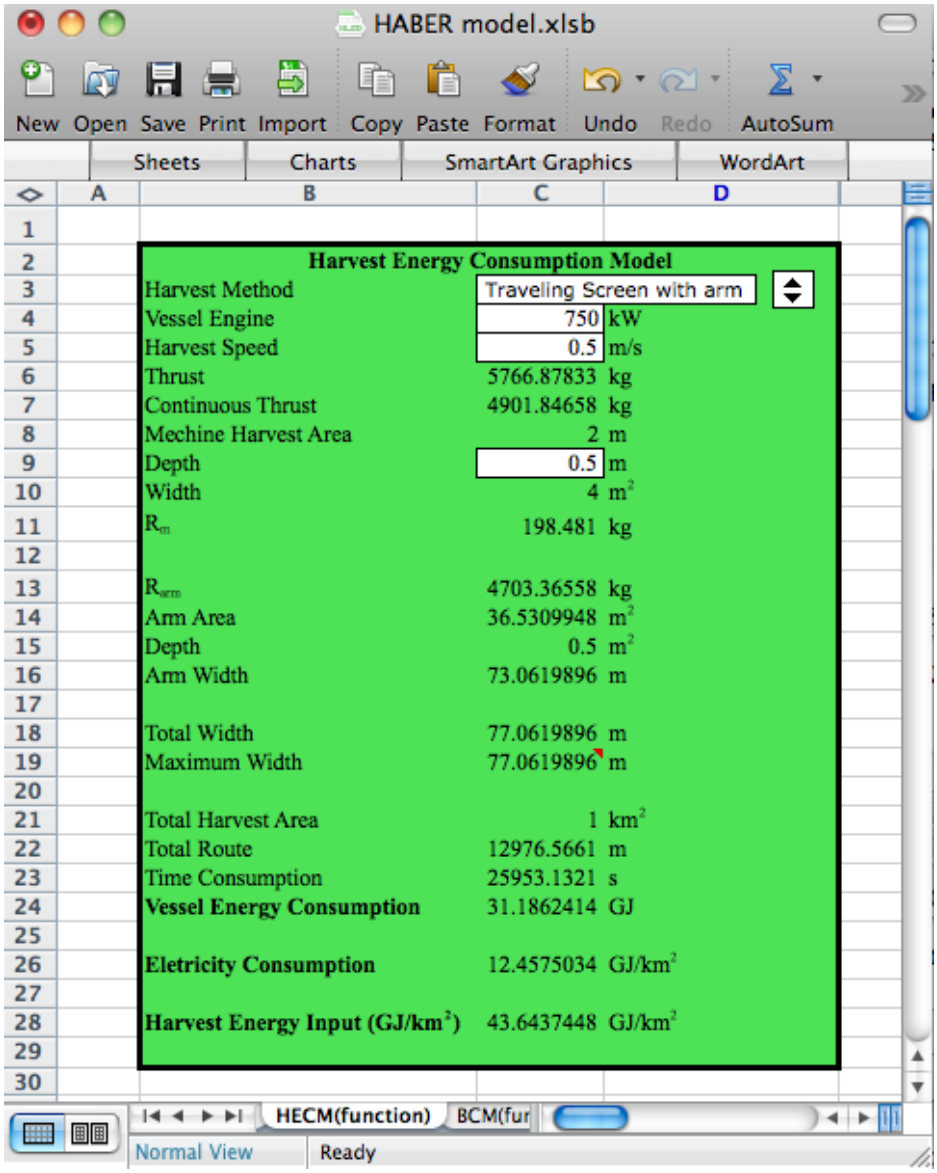

Figure 2-14. Harvest energy consumption model.

2.4.1. Harvest Fuel Consumption

Table 2-3 shows the parameters used in the harvest fuel consumption calculation. The kinetic energy equation (Hwang, 1984) can be used to describe the movement process, shown as Equation (4).

Table 2-3. Vessel parameters.

HECM Vessel Parameters	Symbol	Unit	Default Value	Range	Source
Engine size	P	kW		150~1500	(Bentz, 1997)
Harvest speed	V	m/s		0.5~1.5	(Prado, 1990)
Max speed	V_{max}	m/s	6.17	12~20	(Prado, 1990)
Power/thrust Conversion coefficient	λ	N/kW	11.47		(Hwang, 1984)
Continuous operation factor	n		0.85	0.75~0.9	(Hwang, 1984; Prado, 1990)
Seawater density	ρ	kg/m^3	1030		(Gale and Thomson, 2006)
Drag coefficient	κ		0.82		(McCormick, 1979)
Net porous open area	μ	%	6	1~70	(General Oceanics, Inc, 2010)
Specific consumption of fuel	η	kg/kW-hour	0.23	0.2~0.27	(Prado, 1990)
Diesel heating value	H_{diesel}	MJ/L	38	36~38	(Clarens and White, 2010)
Engine fuel consumption	C	L			
Diesel density	ρ_{diesel}	kg/L	0.84		
Machine harvest area	A_m	m^2			
Harvest area	A_h	m^2			
Vessel energy consumption	E_h	MJ			

$$\Gamma = R_s + R_m + R_{arm} \tag{4}$$

Where Γ is the thrust provided by engine in N, R_s, R_m and R_{arm} are the resistance caused by ship, harvest machine, and focusing arms. All thrust are used against resistance. Thrust and ship resistance can be further expressed by engine power (P), velocity (V) and the power/thrust conversion coefficient, λ (Hwang, 1984).

$$n\lambda P(1-\frac{V^2}{V_{max}^2}) = R_m + R_{arm} \tag{5}$$

Where n is the continuous operation factor, λ is the coefficient of engine power converting to thrust, in N/kW. It is varies depending on the design of propeller, and is 11.47 for general

fishing boats (Hwang, 1984). P is the engine power in kW. V_{max} is max cruise speed, given 6.17 m/s (12 knots) for near coast fishing boats (Prado, 1990). R_m and R_{arm} are the resistance provide from the harvesting machine and focusing arms, in N.

To calculate the work consumed by the machine resistance, we use the drag equation to calculate the force required to maintain the harvest machine at given speed in the water, shown as Equation (6) (Prado, 1990).

$$R_m = -\frac{1}{2}\rho A_m(1-\mu)V^2\kappa \tag{6}$$

Where ρ is seawater density, A_m represents the cross section area of harvest machine in water. μ is the open area of harvest equipment related to the mesh/screen size. For 10 μm mesh size the open area decrease to 6% (General Oceanics, Inc, 2010). κ is the drag coefficient that is used to quantify the resistance of different shape object in a fluid environment (McCormick and Barnes, 1979). For plankton net, we use long cylinder coefficient 0.82. For traveling screen, we use 1.05 as a cube shape. From Equation (6), the cross section area of harvest machine A_m can be calculated. By given harvest depth D_m and obtain the harvest width W_m.

$$A_m = D_m \times W_m \tag{7}$$

Where A_m is the machine harvest area, in m^2, D_m is the machine harvest depth, in m, W_m is the machine harvest width, in m. With known harvest speed (V) and harvest width (W_m), time (T) required for harvesting unit ocean surface area A_h can be calculated.

$$T = \frac{A_h}{V \times W_m} \tag{8}$$

Based on the fisherman's workbook (Prado, 1990), the fuel consumption by an engine during a given period of time can be described as

$$C = 0.75N\frac{\eta}{D_{diesel}}T \tag{9}$$

Where C is the fuel consumption of the engine in a period of time, in liters. 0.75 is an average coefficient of fuel consumption; free running it is between 0.7 and 0,8 and ranging from 0.5~0.8 with loading (Prado, 1990). P is engine power in kW. η represents the specific fuel consumption of diesel engine, in kg/kW-hour, which indicates the weight of fuel consumption

for 1 kW engine operating 1 hour (Prado, 1990). D_{diesel} is the density of diesel, 0.84 kg/L. Therefore, the fuel energy consumption for harvesting can be expressed as Equation (10)

$$E_{vessel} = C \times H_{diesel} \tag{10}$$

Where E_{vessel} is the total energy consumption of harvesting vessel, in MJ, C is the fuel consumption in liters, H_{diesel} is the heating value of diesel, MJ/L.

2.4.2. Harvesting Machine Energy Consumption

In the HECM, the harvesting machine energy consumption is contributed by: plankton net trawling, traveling screen and the screw pump. Each method has individual parameters to describe energy consumption.

2.4.2.1. Plankton Net Trawling Energy Consumption

The energy consumption for plankton net trawling is comprised of: 1. Energy used for trawling/filtering and 2. Energy used to pull the plankton net up from water and 3. Cleaning by jet water. The first part of the energy use is covered in vessel consumption. Therefore, this part of the model will focus on the energy used for pulling plankton net and jet water pump. The energy used for jet water pump is negligible because the kW of offshore jet water pump is usually less than 0.75 kW (BPS, 2010). The parameters used for plankton net energy consumption are shown in Table 2-4.

Table 2-4. Plankton net parameters.

Plankton Net Parameters	Symbol	Unit	Default Value	Range	Source
Net diameter	D_{net}	m	0.5	0.3~5	(General Oceanics, Inc, 2010)
Net L/D ratio	α		3	3~9	(General Oceanics, Inc, 2010)
Boat deck height	h	m	5	1~10	(East Coast Marine, 2010)
Clogging Time	τ	minutes	10	10~100	(Smith et al., 1968)
Generator efficiency	ε		0.6	0.8~0.4	(James, 2005)
Harvest energy consumption	E_h	MJ/km^2			

To estimate the energy use for pulling up water, we apply the potential energy equation (Smith and Crosbie, 1998).

$$U = mgh \tag{11}$$

Where U is the potential energy in kJ, m is the mass of the pull up water in kg, g is the gravity, 9.8 m/s^2, h is the water head of moving water from ocean surface onto the boat. To calculate the mass of the plankton net, we are assuming to use cone shaped plankton nets with the diameter (D_{net}) equal to harvest depth. The general length to diameter ratio (α) for plankton net is usually from 3 to 6 (General Oceanics, Inc, 2010). Hence we can calculate the volume of single plankton net (V_{net}) as a cone shape object (Russel, 2010).

$$V_{net} = \frac{\alpha \pi D_{net}^3}{12} \tag{12}$$

Where V_{net} is the volume of the plankton net, in m^3, α is the net length/diameter ratio, D_{net} is the net diameter, in meters. We can calculate the number of plankton nets (N_{net}) by dividing the machine harvest area (A_m) by the plankton net mouth open area (A_{net}).

$$N_{net} = \frac{A_m}{A_{net}} = \frac{4A_m}{\pi D_{net}^2} \tag{13}$$

Based on the Equation (12), (13), and (14), we can calculate the energy required for pulling up plankton nets one time by given h as boat height.

$$U = V_{net} N_{net} gh \tag{14}$$

For 10 μm mesh size plankton net, the open area is 6% (General Oceanics, Inc, 2010). Thus, the model use 6% open area to adjust reference area. The filtration efficiency of plankton net usually starts at 90% and decrease over time because of fouling (Smith et al., 1968). The fouling rate is closely related to the mesh size and particle concentration in water. A 20 μm mesh size plankton net will clog in ten minute (Smith et al., 1968). Therefore, preparation of another set of plankton nets is recommended, as it can avoid spending time on waiting for cleaning the net.

$$E_h = \frac{TU}{\tau \varepsilon} \tag{15}$$

Where E_h is the energy consumption. ε is the generator efficiency (0.6), τ is the clogging time, given 10 minutes, T is the time required to harvest a unit ocean surface, in minutes and U is the energy consumption each time, in kJ. Assuming to use a generator for powering the harvest machine, generator efficiency (ε) of converting fuel energy into electricity is included in the calculation.

2.4.2.2. Traveling Screen Energy Consumption

The energy used for the traveling screen is based on the assumption that we install the AlgaeVenture System, Harvest Dewatering Drying (AVSHDD) machine on the boat and use it to harvest algae. It has been proved that it can harvest algae in a lake (AVS, 2010). The energy consumption used in the model is according to the data provided by the company. The parameters used for traveling screen energy consumption are shown in Table 2-5.

Table 2-5. Traveling screen parameters.

Traveling Screen Parameters	Symbol	Unit	Default Value	Range	Source
Screen harvest area	A_{screen}	m^2			
Harvest speed	V	m/s	0.5	0.5~1.5	(Prado, 1990)
Harvest time	T	second			
HDD harvest efficiency	δ	$kJ/m^3 \cdot hour$	288		(AVS, 2010)
Generator efficiency	ε		0.6	0.8~0.4	(James, 2005)
Harvest energy consumption	E_h	MJ/km^2			

We test two different scenarios in this model. The first scenario is similar to the algae harvester developed by Simplexity Creative (2010), coupling traveling screens in a row, shown as Figure 2-15. It requires a large number of filer membrane units to achieve wide range harvesting. Therefore, second scenario that combines HDD with focusing arm. Given the machine harvest area, we can vary the focusing arm width to achieve max harvest area.

Figure 2-15. Algae harvester developed by Simplexity Creative (2010).

The information of AVSHDD system energy consumption is provided by the manufacture, which is 288 kJ per cubic meter water processed (AVS, 2010). The machinery energy consumption can be calculated by the amount of processing water. The condition can be describe by Equation (16)

$$E_h = \frac{A_{screen} VT\delta}{\varepsilon} \tag{16}$$

Where E_h is the energy used for harvesting, in kJ, and A_{screen} is the area of screen submerged in water, in m^2. In the first scenario, A_{screen} equals the max harvesting area. For scenario 2, A_{screen} is a given value, 4 m^2 is used as a default value, V is harvesting speed in m/s, T is the harvesting time, in hour, δ is AVSHDD energy consumption efficiency in $kJ/m^3 \cdot hour$, ε is the generator efficiency.

2.4.2.3. Screw Pump Energy Consumption

To describe the energy consumption for screw pump, first we need to calculate the power applied to water (P_w) as it moves through the pump up to the deck height (h), shown as Equation (17) (Aarne et al., 1994). The parameters used in screw pump energy consumption calculation are shown as Table 2-6.

Table 2-6. Screw pump parameters.

Screw Pump Parameters	Symbol	Unit	Default Value	Range	Source
Power applied on water	P_w	kW			
Flow rate	Q	m^3/s			
Boat deck height	h	m	3	2 ~ 10	(East Coast Marine, 2010)
Screw pump efficiency	ψ		0.6	0.9~0.4	(Burenin, 2002)
Generator efficiency	ε		0.6	0.8~0.4	(James, 2005)
Harvest energy consumption	E_h	MJ/km^2			

$$P_w = 1000Qgh \tag{17}$$

Where P_w is the power apply on water for lifting, in kW, 1000 is a conversion coefficient that converting cubic meter water to kg, and Q is the flow rate in m^3/s. In the model, the flow rate is affected by the machine harvest area (A_h) and harvest speed (V). h is the lifting distance,

deck height in this case. Equation (17) provides the energy consumed for moving water. However, the actual power required to run a pump will be higher because the pump is not 100 percent efficient. Therefore, screw pump efficiency is added into the Equation (18)

$$P_{pump} = \frac{P_w}{\psi} \tag{18}$$

Where P_{pump} is the screw pump power required to lift water, in kW, ψ is the screw pump efficiency. The energy consumption of the screw pump is expressed as the Equation (19)

$$E_h = \frac{P_{pump} \times T}{\varepsilon} \tag{19}$$

Where E_h is the energy used for harvesting, in kJ, P_{pump} is the screw pump power required to lift water, in kw, T is harvest time, in seconds, ε is the generator efficiency.

2.5. Biofuel Conversion Model

The second sub-model, the biofuel conversion model is used to compare the net energy production of four different conversion technologies. They are hydrothermal liquefaction, anaerobic digestion, transesterification and fermentation. The process scheme is shown in Figure 2-16. This model contains two major parts. The first part is estimating the energy consumption of each transformation process. The second part is modeling the amount of biofuel production. Therefore, the net energy production and the energy input/output ratio can be obtained from the model.

The BCM model is also present in the EXCEL worksheet. Figure 2-17 shows the interface of the model. The user is required to type in the algae sample biochemical composition and select a conversion method. BCM will present the energy production, pretreatment energy input, conversion energy input, net energy production and energy ratio.

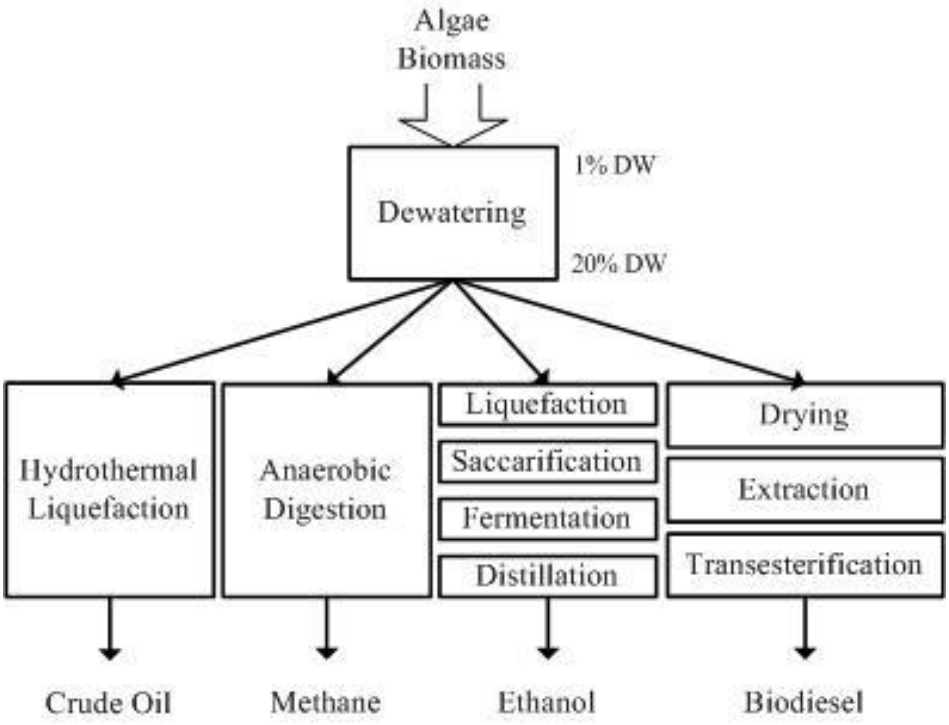

Figure 2-16. Biofuel conversion model scheme.

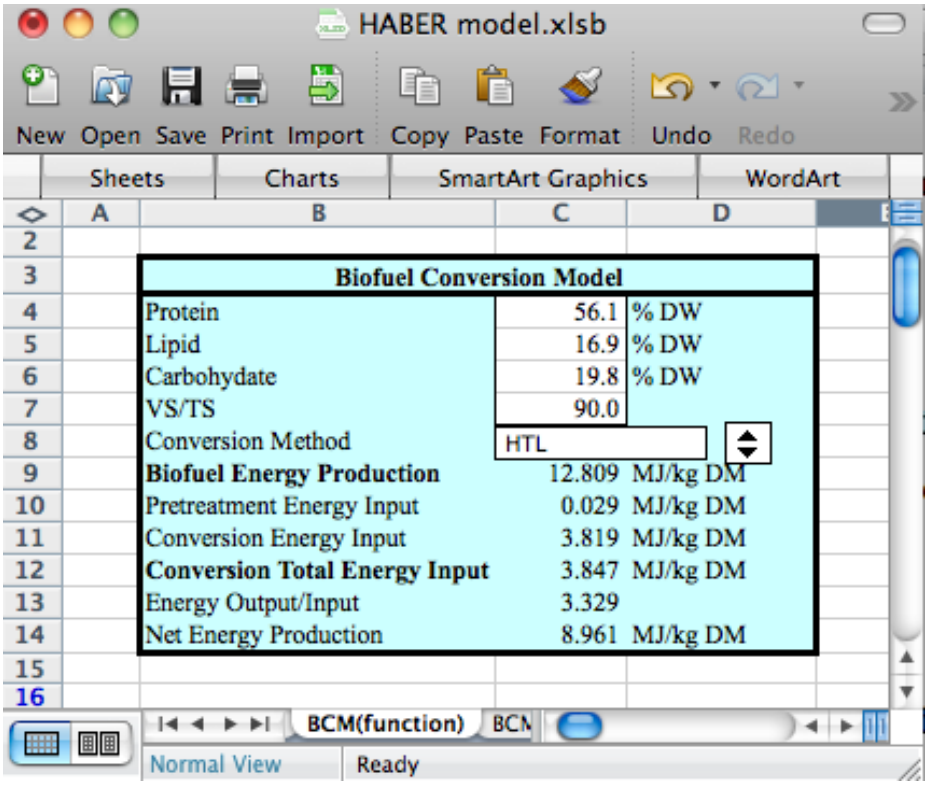

Figure 2-17. Biofuel conversion model interface.

2.5.1. Hydrothermal Liquefaction Energy Consumption

Hydrothermal conversion is the process that converts organic matters into synthesis gas, crude oil or char through high pressure, temperature and small amount of catalyst (Tsukahara and Sawayama, 2005). Based on the main products, hydrothermal conversion can be categorized into gasification, pyrolysis, and liquefaction. Liquefaction is a hydrolyzed thermochemical reaction. This process transforms organic matter into bio-crude oil. It is usually processed under 5-20 MPa pressure and 250-350^{o}C. In most instances, pretreatment is needed before conversion. Feedstock should be homogenized and adjusted moisture content between 20~50%. Studies of algal biomass liquefaction have been documented. In Yang's study showed *Microcystis viridis* under 3MPa, 340℃ and 5% Na_2CO_3 for 30 min have the 33% oil production and the heating value of oil is 31 MJ/kg (Yang et al., 2004). Other researchers tested *Botvyococcus braunii* biomass liquefaction in the condition of 2MPa, 300℃ and 5% Na_2CO_3 for 1 hour (Dote et al, 1994). The result shows 64 wt% of oil produced and a heating value of 49 MJ/kg. Minowa performed *Dunaliella tertiolecta* liquefaction at 340℃, 10 MPa for 1 hour and obtain 37% oil yield. The oil heating value is 36 MJ/kg (Minowa et al., 1995).

In the Biofuel Conversion Model, the energy consumption for hydrothermal liquefaction is shown in Figure 2-18.

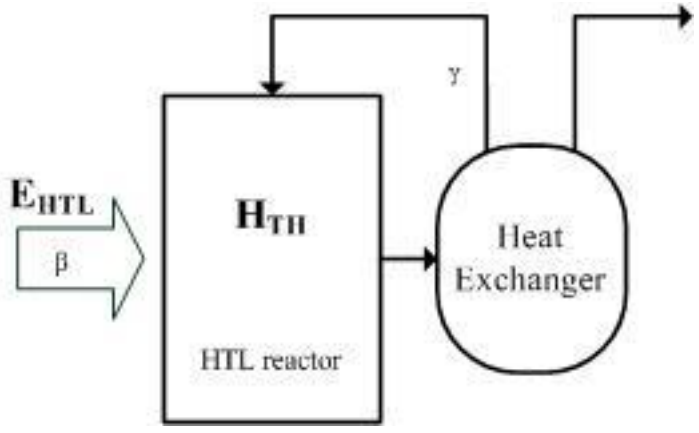

Figure 2-18. HTL energy consumption.

Based on Sawayama's study, the theoretical energy consumption of liquefaction is calculated by Equation (20) (Sawayama et al., 1999). Table 2-7 shows the parameters of HTL energy consumption.

Table 2-7. HTL energy consumption parameters.

HTL Consumption Parameters	Symbol	Unit	Default Value	Range	Source
Solid content	ϕ	kg/kg	0.2	0.1~0.3	(Robertson and Lasala, 1992)
Specific heat of water	μ_w	kJ/kg· °C	4.18		(Sawayama et al., 1999)
Specific heat of solid	μ_s	kJ/kg· °C	1.25		(Sawayama et al., 1999)
Reaction temperature	T_R	°C	280	250~350	(Peterson et al., 2008)
Heat recovery efficiency	γ		0.5	0.9~0.2	(Sawayama et al., 1999)
Combustion efficiency	β		0.6	0.8~0.4	(Sawayama et al., 1999)
Theoretical energy input	H_{TH}	kJ/kg D.A.			(Peterson et al., 2008)
Energy consumption	E_{HTL}	kJ/kg D.A.			

$$H_{TH} = \frac{(1-\phi)\mu_w(T-25) + \phi\mu_s(T-25)}{\phi} \tag{20}$$

Where H_{TH} is the theoretical energy consumption of HTL, kJ/kg dry algae, T_R is the reaction temperature, in °C, ϕ is the solid content of HTL feedstock, μ_w is the specific heat of water, 4.18 kJ/kg· °C, μ_s is the specific heat of water, 1.25 kJ/kg·°C (Sawayama et al., 1999).

To estimate the energy consumption for a more practical condition, we also consider combustion efficiency and heat recovery rate in this model, shown as Figure 2-18. Based on Figure 2-18, the energy input of HTL reaction can be written as Equation (21).

$$E_{HTL} = \frac{H_{TH}}{\beta}(1-\gamma) \tag{21}$$

Where E_{HTL} is the energy consumption of HTL per kg dry algae processed, in kJ/kg, H_{TH} is the theoretical energy consumption of HTL, kJ/kg dry algae, β is combustion efficiency that combustor transfer the heat to reactor, assumes 0.6 (Sawayama et al., 1999). γ is the heat recovery efficiency, assumes 0.5 (Sawayama et al., 1999).

2.5.2. Hydrothermal Liquefaction Energy Production

Although HTL has been developed for decades, in terms of industrial applications, it is still a relatively novel technology for algae biofuel production. Early efforts were focused on waste biomass conversion. Therefore, the research concerning the relationship between algae composition and oil production is limited. Biller has touched on the modeling of crude oil production by the biochemical compositions (Biller and Ross, 2010). However, the author does not provide the modeling value due to low fitness to cyanobacteria. Therefore, in this HTP production model, we adapted a series of HTL experiments performed by University of Illinois, Dr. Zhang Yuanhui's group, and used a linear regression method to determine conversion coefficient for each component. Table 2-8 shows the parameters for HTL crude oil energy production. Equation (22) is used for predicting crude oil production (Biller and Ross, 2010).

Table 2-8. HTL biocrude oil production parameters.

HTL Production Parameters	Symbol	Unit	Default Value	Range	Source
Algae protein content	χ_P	g/g D.A.(%)	30	20~63	(Beker, 2006)
Algae lipid content	χ_L	g/g D.A.(%)	18	6~46	(Mata et al., 2010)
Algae carbohydrate content	χ_C	g/g D.A.(%)	28	6.9~45	(Gladue and Maxey, 1994)
Algae ash content	χ_A	g/g D.A.(%)	10	7.2~39	(Gladue and Maxey, 1994)
Protein coefficient	P_{HTL}	kg/kg pro.	0.401		This study
Lipid coefficient	L_{HTL}	kg/kg lipid	0.668		This study
Carbo. coefficient	C_{HTL}	kg/kg carb.	0.31		This study
Ash coefficient	A_{HTL}	kg/kg ash	-0.225		This study
Crude oil heating value	H_{crude}	MJ/kg oil	34	32~45	(Biller and Ross, 2010)
HTL energy yield	Y_{HTL}	MJ/kg D.A.			

$$Y_{HTL} = (P_{HTL}\chi_p + L_{HTL}\chi_L + C_{HTL}\chi_C + A_{HTL}\chi_A)H_{crude} \quad (22)$$

Where Y_{HTL} is the energy yield of HTL crude oil per kg dry algae, in MJ/kg, χ_P is the protein content of dry algal biomass, range from 20 to 63% (Beker, 2006), P_{HTL} is the conversion coefficient of proteins convert into crude oil, 0.401 by experiments results, χ_L is the lipid content of dry algal biomass, range from 6 to 46% (Mata et al., 2010), L_{HTL} is the conversion coefficient of lipids convert into crude oil, 0.668 by experiments results, χ_C is the carbohydrate content of dry algal biomass, range from 6.9 to 45% (Gladue and Maxey, 1994), C_{HTL} is the conversion

coefficient of carbohydrates convert into crude oil, χ_A is the ash content of dry algal biomass, range from 7.2 to 39% (Gladue and Maxey, 1994), A_{HTL} is the conversion coefficient of ash affects on crude oil production, -0.225 by experiments, H_{crude} is the heating value of crude oil, range from 32 to 45 MJ/kg (Biller and Ross, 2010)

2.5.3. Anaerobic Digestion Energy Consumption

Anaerobic digestion is a biochemical process that converts organic matter into biogas under no oxygen condition. The conversion process includes complex microorganism interaction, which can be categorized into three processes: hydrolysis, acetogenesis and methanogenesis (Brennan and Owende, 2010). Hydrolysis degrades complicated components like carbohydrates, proteins, and lipids into small molecular compounds such as sugars, ammonia and organic acid. Fermentative bacteria then convert these small molecules into alcohols, carbonic acid, hydrogen and carbon dioxide. The final stage of anaerobic digestion is methanogenesis. Methanogens convert the intermediate products from the previous stage into methane and CO_2 gas, which is the main component in biogas.

In comparison to other conversion technologies, anaerobic digestion is a low energy input process. In the Biofuel Energy Consumption model, we assume the major energy input components of anaerobic digestion are the dewatering process and the energy used for the anaerobic digester. The dewatering process is assumed to use AVSHDD process to dry algae from 1% solid content to 20% solid content (AVS, 2010). Berglund's study (2006) shows the energy demand for a pilot scale anaerobic digester (20,000 ton/year) is 1.8~0.7 MJ/kg, and 0.66 MJ/kg for electricity. Chisti (2008) estimated the energy consumption for algae biomass anaerobic digestion to be 1.1 MJ/kg dry biomass. In Bohn's study (2007), energy consumption for digester is 2.5~1.65 MJ/kg dry biomass. In HECM model, the main energy consumed components are dewatering machines and anaerobic digester, shown as Equation (23). The parameters of anaerobic digestion energy consumption are shown in the Table 2-9.

Table 2-9. Anarobic digestion consumption parameters.

AD Consumption Parameters	Symbol	Unit	Default Value	Range	Source
Energy for dewatering	$E_{dewater}$	MJ/kg D.A.	0.0029		(AVS, 2010)
Energy for anaerobic digester	$E_{digester}$	MJ/kg D.A.	2	1.1~2.5	(Chisti, 2008; Bohn et al., 2007)
AD total energy consumption	E_{AD}	MJ/kg D.A.			

$$E_{AD} = E_{dewater} + E_{digester} \quad (23)$$

Where E_{AD} is the energy consumption of anaerobic digestion, in MJ/kg dry algae, $E_{dewater}$ is the energy consumption of dewatering process, 0.0029 MJ/kg dry algae (AVS, 2010), $E_{digester}$ is the energy consumption of digester, in the range of 1.1 to 2.5 MJ/kg dry algae (Chisti, 2008; Bohn et al., 2007).

2.5.4. Anaerobic Digestion Energy Production

In the general scheme for anaerobic digestion, feedstock is loaded into a digester and maintained at a temperature at 35 ^{o}C, and has active inoculums of microorganisms required for the methane fermentation. The hydraulic retention time should be adjusted base on feedstock water content. For diluted low solids (<1%) biomass, attached-film reactors are employed. Attachment of organisms on to inert media permits low retention time (<1day) without wash out. For intermediate solids (5-10%) feedstock, solids and organisms are recycled following settling within the digester or in a separate secondary digester. Saline water may cause inhibition in an anaerobic digestion process. Riffat's study shows the reactor that is mixing anaerobic sludge with halophilic methanogenes can operate at 35 g/L sodium chloride concentration (Riffat and Krongthamchat, 2007). There are many studies that have documented algae biomass anaerobic digestion. Samson uses 2% *Spirulina maxima* as feedstock (Samson and Leduy, 1986), the result shows that methane production is 0.35 m^3 per kg volatile solid (VS) per day at 11 days retention time. Morand tested the performance of anaerobic digestion of macroalgae *Ulva sp.2*. The study processed biomass in the retention time of five days and had a methane yield 0.33 m^3 per kg volatile biomass per day (Morand and Briand, 1999). Yen and Brune mix waste paper with algae to adjust the C/N ratio and have significant improvement from 0.15 m^3/kg(VS)·day to 0.29 m^3/kg(VS)·day (Yen and Brune, 2007).

To estimate the methane production from anaerobic digestion in the model, we investigate the anaerobic digestion model from previous literature. Karpenstein-Machan tested the specific methane yield of crude protein, crude oil, and carbohydrates (Karpenstein-Machan, 2005). The results were 490 L/kg(VS), 850 L/ kg(VS) and 395 L/kg(VS), respectively. Bruno developed a methane yield model based on the elements percentage (Sialve et al., 2009). He calculated the elements percentage of proteins, lipids, and carbohydrates and gave the theoretical components of methane production, which is 851, 1031, 415 L/kg(VS). Amon tested the methane yield coefficients of different biomass feedstock. For example, the coefficients of maize crude protein, crude oil and crude fiber are 15.27, 28.38 and 4.54, respectively, whereas the coefficients for grass are 2.19, 31.38 and 1.48 (Amon et al., 2007). This result suggests that crude fat is the major component affecting methane production. However, the conversion coefficients are feedstock related. Briand estimated the methane yielding potential coefficients of algae biomass, which are 400 × (%carbohydrate) + 400 × (%protein)+ 900× (%lipids) in L/kg(VS) (Briand, 1997). Since this was the only study we found describing the methane yield from algal biomass, we adopted this model for our methane yielding equation, shown as Equation (24) (Briand, 1997). The probable volatile solids destruction percentage is between 35~60% (Barker, 2001). Therefore, we include digestion percentage (Ω) in the equation. Parameters for anaerobic digestion production model are showed in Table 2-10.

Table 2-10. Anaerobic digestion production parameters.

AD Production Parameters	Symbol	Unit	Default Value	Range	Source
Algae protein content	χ_P	g/g D.A. (%)	30	20~63	(Beker, 2006)
Algae lipid content	χ_L	g/g D.A. (%)	18	6~46	(Mata et al., 2010)
Algae carbohydrate content	χ_C	g/g D.A. (%)	28	6.9~45	(Gladue and Maxey, 1994)
Protein coefficient	P_{AD}	L/kg protein	400	400	(Briand, 1997)
Lipid coefficient	L_{AD}	L/kg lipid	900	900	(Briand, 1997)
Carbohydrate coefficient	C_{AD}	L/kg carbo.	400	400	(Briand, 1997)
Digestion percentage	Ω		0.5	0.3~0.7	(Barker, 2001)
Methane heating value	$H_{methane}$	kJ/L methane	37	36~40	
Methane energy yield	Y_{AD}	MJ/kg D.A.			

$$Y_{AD} = (P_{AD}\chi_p + L_{AD}\chi_L + C_{AD}\chi_C)\Omega H_{methane} \quad (24)$$

Where Y_{AD} is the energy yield of anaerobic digestion per kg dry algae, in MJ/kg, χ_P is the protein content of dry algal biomass, range from 20 to 63% (Beker, 2006), P_{AD} is the conversion coefficient of proteins convert into methane, in L/kg protein, χ_L is the lipid content of dry algal biomass, range from 6 to 46% (Mata et al., 2010), L_{AD} is the conversion coefficient of lipids convert into methane, in L/kg lipid, χ_C is the carbohydrate content of dry algal biomass, range from 6.9 to 45% (Gladue and Maxey, 1994), C_{AD} is the conversion coefficient of carbohydrates convert into methane, in L/kg, Ω is the digestion percentage, varies with reaction time and condition, $H_{methane}$ is the heating value of methane, range from 36 to 40 MJ/L

2.5.5. Transesterification Energy Consumption

Transesterification is the processing of triglycerides with an alcohol to form esters and glycerol. The whole reaction includes three reversible steps, as shown in Figure 2-19. Triglycerides are converted to diglycerides, then converted into monoglycerides. Monoglycerides are then reacted with alcohol and form the mono-alkyl ester (biodiesel), and glycerol (Hossain et al. 2008). Although the alcohol: oil theoretical molecular ratio is 3:1, it is common to use 6:1 to complete the reaction accurately. Methanol and ethanol are the most common alcohol used in transesterification. Potassium hydroxides or sodium hydroxides are used as catalyses to provide high pH environment for reaction.

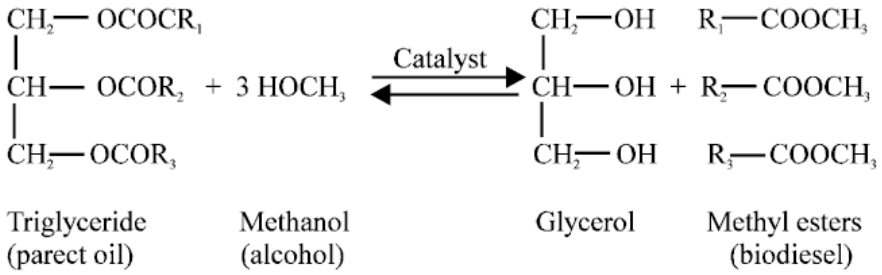

Figure 2-19. Transesterification reaction (Hossain et al., 2008).

Figure 2-20 gives an overview of the transesterification process chain (Mata et al., 2010). The first step after harvesting algae biomass is dewatering the sludge from 1% to 20% solid content. Following the dewatering process, the algae biomass must be dried to higher than 90% through a drying process. In Lardon's study, the energy required to dry algae biomass from 80%

water to below 10% is 14.1 MJ/kg dry biomass (Lardon et al., 2009). This value corresponds to Chisti's result of 15.85 MJ/kg dry biomass (Chisti, 2008). Lipid extraction is then applied to the biomass for lipid separating. In this model, we assume a solvent extraction since it is commercialized. The energy consumption is 1.24 MJ/kg dry biomass (Lardon et al., 2009). Lipids are extracted, and then processed by transesterification for biodiesel production. The energy consumption for transesterification is 0.9 MJ/kg dry biomass (Lardon et al., 2009). To calculate the energy consumption of biodiesel production process, we include four major energy consumed processes in the Equation (25) based on the Figure 2-20 (Meta et al., 2010). The parameters used for Equation (25) are shown in Table 2-11.

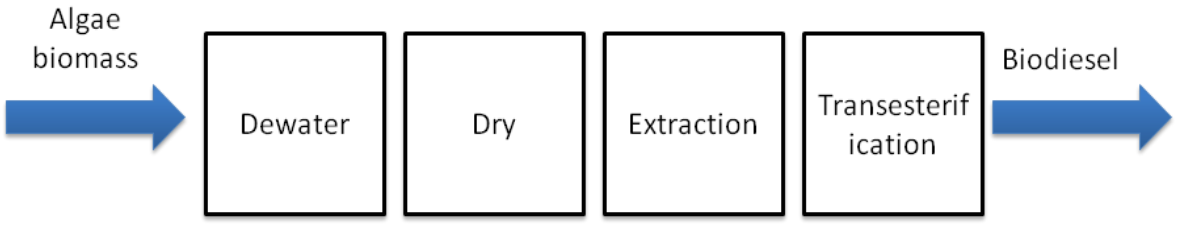

Figure 2-20. Transesterification process (Mata et al., 2010).

Table 2-11. Transesterification energy consumption parameters.

Trans Consumption Parameters	Symbol	Unit	Default Value	Range	Source
Energy for dewatering	$E_{dewater}$	MJ/kg D.A.	0.29		(AVS, 2010)
Energy for drying	E_{dry}	MJ/kg D.A.	13	11~15	(Chisti, 2008; Lardon et al., 2009)
Energy for extraction	$E_{extraction}$	MJ/kg D.A.	1.24		(Lardon et al., 2009)
Energy for transesterification	E_{trans}	MJ/kg D.A.	0.9		(Lardon et al., 2009)
Trans total energy consumption	E_{TTrans}	MJ/kg D.A.			

$$E_{TTrans} = E_{dewater} + E_{drying} + E_{extraction} + E_{trans} \quad (25)$$

Where E_{TTrans} is the total energy consumption of biodiesel produced from algal biomass, in MJ/kg dry algae, $E_{dewater}$ is the energy consumption of dewatering process, 0.0029 MJ/kg dry algae (AVS, 2010), E_{drying} is the drying process energy consumption, 13 MJ/kg dry algae (Chisti,

2008), $E_{extraction}$ is the energy consumption of extraction, 1.24 MJ/ kg dry algae biomass (Lardon et al., 2009), E_{trans} is the energy consumption of transesterification reaction, 0.9 MJ/kg dry algae (Lardon et al., 2009).

2.5.6. Transesterification Energy Production

Transesterification can only convert lipids into biofuel. Hexane extraction is currently the most efficient method to separate lipid from the other components, the extraction efficiency is 92.5% (Sander and Murthy, 2010). Transesterification can convert 99% of algal oil into biodiesel (Sander and Murthy, 2010). The heating value of algae oil converted biodiesel is in the range of 36 to 40 MJ per kg biodiesel (Chisti, 2008; Minowa et al., 1995;Vijyaraghavan and Hemanathan, 2009). Based on Sander and Murthy's study (2010), transesterification yield can be described as Equation (26) and parameters are shown in Table 2-12.

Table 2-12. Transesterification biodiesel production parameters.

Trans Production Parameters	Symbol	Unit	Default Value	Range	Source
Algae lipid content	χ_L	g/g D.A. (%)	18	6~46	(Meta et al., 2010)
Extraction efficiency	σ	%	92.5		(Sander and Murthy, 2010)
Transesterification efficiency	ω	%	99		(Sander and Murthy, 2010)
Biodiesel heating value	$H_{biodiesel}$	MJ/kg	38	36~40	(Chisti, 2008; Minowa et al., 1995; Vijyaraghavan and Hemanathan, 2009)
Biodiesel energy yield	Y_{trans}	MJ/kg D.A.			

$$Y_{trans} = \sigma\omega\chi_L H_{biodiesel} \quad (26)$$

Where Y_{trans} is the biodiesel energy production from 1 kg of dry algal biomass, in MJ/kg, σ is the extraction efficiency of hexane extraction, assumes 92.5% (Sander and Murthy, 2010), ω is the transesterification efficiency that converts extracted algal oil into biodiesel, assumes 99% (Sander and Murthy, 2010), $H_{biodiesel}$ is the heating value of biodiesel, in the range of 36 to 40 MJ/kg (Chisti, 2008; Minowa et al., 1995; Vijyaraghavan and Hemanathan, 2009).

2.5.7. Fermentation Energy Consumption

Fermentation is a biological conversion process similar to anaerobic digestion. However, yeast is the major organism that converts carbohydrates like sugar, starch or cellulose into ethanol. Since currently there is no ethanol plant that uses algae biomass as feedstock, we adopt corn ethanol energy consumption data and adjusted the value base on the starch content. In the model, the harvested biomass needs to be dewatered through AVSHDD system to achieve 80~70% of moisture content for the liquefaction process (AVS, 2010). The major energy usage during liquefaction is to heat up feedstock to 80 °C. The energy consumption is 2.81 MJ/L ethanol (Mei et al., 2009). Assuming corn starch content is 60% and 100% (w/w) of starch is converted into ethanol, the energy consumption for 1 kg feedstock liquefaction is 1.69 MJ/kg dry biomass. The saccharification process and fermentation require very low energy input since they react at room temperature. Therefore, the energy consumption for these two processes can be neglected. The other major energy consumption of fermentation is distillation. Based on the study by Cardona et al. (2006), the energy input for distillation is 8.229 MJ/kg D.A. Where Mei et al. (2009) study indicates 7.05 MJ/kg dry algae is required for distillation. Equation (27) and Table 2-13 are used to describe the energy consumption of the fermentation process.

Table 2-13. Fermentation energy consumption parameters.

Fermentation Consumption Parameters	Symbol	Unit	Default Value	Range	Source
Energy consumption of liquefaction	E_{liq}	MJ/kg D.A.	1.69		(Mei, et al., 2009)
Energy consumption of distillation	E_{distil}	MJ/kg D.A.	7.5	7.05~8.23	(Mei et al., 2009;Cardona et al., 2006)
Energy consumption of fermentation	$E_{ferment}$	MJ/kg D.A.			

$$E_{ferment} = E_{liq} + E_{distil} \quad (27)$$

Where $E_{ferment}$ is the energy consumption of the whole fermentation process, in MJ/kg dry algae, E_{liq} is the energy consumption of liquefaction, 1.69 MJ/kg dry algae (Mei, et al., 2009), E_{distil} is the energy consumption of distillation process, in the range of 7.05 to 8.23 MJ/kg dry algae (Mei et al., 2009;Cardona et al., 2006).

2.5.8. Fermentation Energy Production

Current ethanol fermentation techniques can convert up to 95% (weight) of the available carbohydrate into ethanol (Feinberg, 1984). Therefore, the main parameter determining ethanol production is the available carbohydrate percentage. Algae carbohydrate content are typically complex mixtures of mono-, poly- and oligosaccharides with pentoses and hexoses having been identified (Feinberg, 1984). The reasonable approach is to assume that about 0.33-0.66 of the carbohydrates can be hydrolyzed to fermentable hexose and the remaining portion goes to pentose (Feinberg, 1984). These assumptions result in a net ethanol production of 0.3-0.6 kg/kg carbohydrates. Hirano (1997) studied the conventional fermentation conversion rate while using microalgae as feedstock. The test showed 37% of carbohydrate can be converted into ethanol. He also calculated a theoretical conversion value of 65%. Algae carbohydrate content was between 2-45%, mostly near 30% (Hirano et al., 1997). Therefore, we assume available carbohydrate is 0.4, in the range of 0.33~0.66. Equation (28) and Table 2-14 described the ethanol yielding.

Table 2-14. Fermentation ethanol production parameters.

Fermentation Production Parameters	Symbol	Unit	Default Value	Range	Source
Algae carbohydrate content	χ_C	g/g D.A.	28	15~64	(Hirano et al., 1997;Gladue and Maxey, 1994)
Available carbohydrate percentage	α_{carbo}	g/g carbo. (%)	40	33~66	(Hirano et al., 1997)
Ethanol conversion Rate	$\beta_{ferment}$	g/g a.carbo.	0.95		(Feinberg, 1984)
Ethanol heating value	$H_{ethanol}$	MJ/kg fuel	29.7		
Ethanol energy yield	$Y_{ferment}$	MJ/kg D.A.			

$$Y_{ferment} = \alpha_{carbo}\beta_{ferment}\chi_C H_{ethanol} \quad (28)$$

Where $Y_{ferment}$ is the energy yield of the ethanol produced from 1 kg algal biomass, in MJ/kg, α_{carbo} is the available carbohydrate percentage, 33~66% (Hirano et al., 1997), $\beta_{ferment}$ is the coefficient of converts available carbohydrates into ethanol, 0.95 (Feinberg, 1984), χ_C is the carbohydrate content in dry algae, 15~ 64 % (Gladue and Maxey, 1994), $H_{ethanol}$ is the heating value of ethanol, 29.7 MJ/kg.

3. RESULTS AND DISCUSSION

3.1. Gulf of Mexico Algae

Figure 3-1 shows the typical annual variation in the amount of algal biomass in the Northern Gulf of Mexico in the areas where the surface chlorophyll concentration as determined by satellite imagery was 3 mg/m^3. The total area above this chlorophyll level is also shown in Figure 3-1. These chlorophyll concentrations were converted into biomass based on long-term monthly average of the algal species composition and the average chlorophyll content of the major species types. By summing up the total chlorophyll in the study area, late April and December appear to be the highest biomass months. About 200,000 metric ton of dry algal biomass is estimated in the field. The lowest biomass estimate is about 80,000 metric ton. February has only one data point due to cloudy weather. It must be noted that the species composition has a huge impact on converting chlorophyll data into biomass. Therefore, community composition and individual species' chlorophyll/biomass ratio should be further studied for refining the accuracy of model prediction accuracy. Figure 3-2 shows the size differences of high chlorophyll density (>7 mg/m^3) area in the Atchafalaya and Mississippi delta regions as well as the total for the both areas. The Atchafalaya and Mississippi deltas are the most eutrophic regions in the Gulf of Mexico. Figure 3-3 shows the total biomass in high density areas in the Atchafalaya and Mississippi delta regions. The total size of these high-density areas is between 600 to 3,200 km^2. The biomass estimation varies between 500 and 9,000 metric tons over the course of the year.

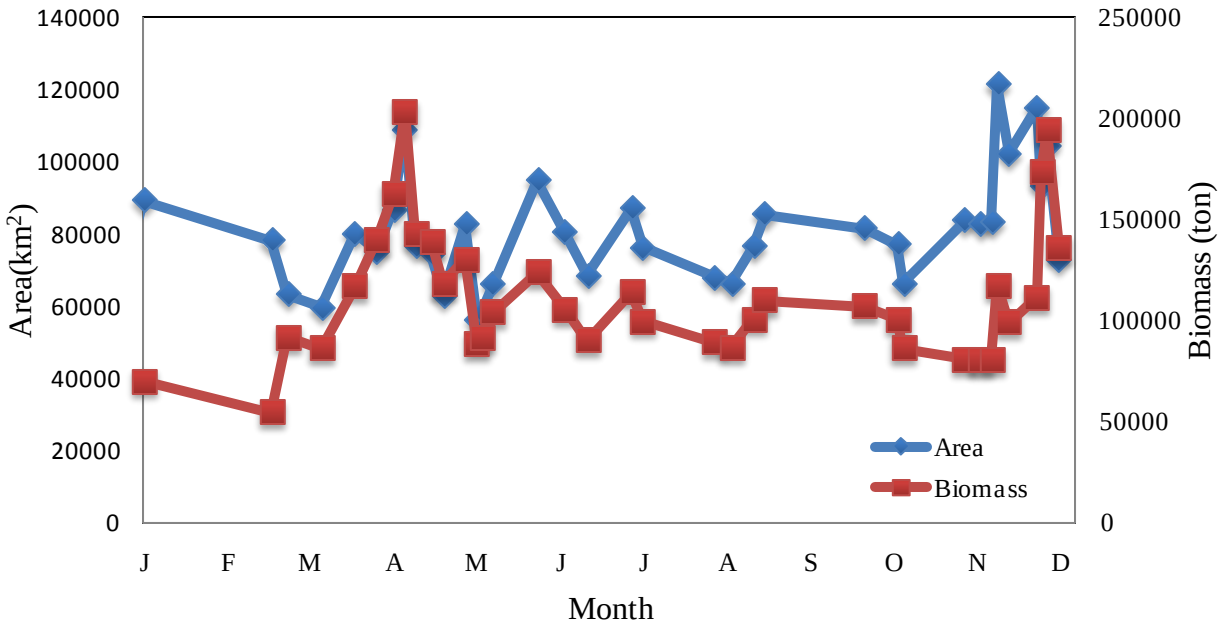

Figure 3-1. 2007 Estimated algal biomass and bloom area in the Gulf of Mexico by sea-WiFS adjusted by algal species composition.

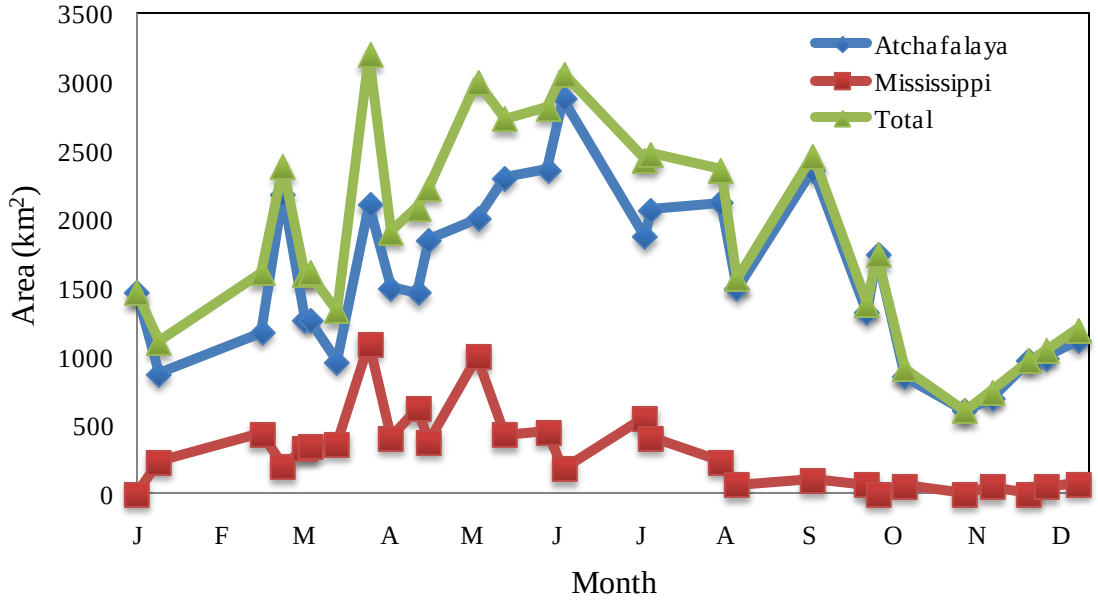

Figure 3-2. 2007 Atchafalaya region and Mississippi region estimated algal bloom area.

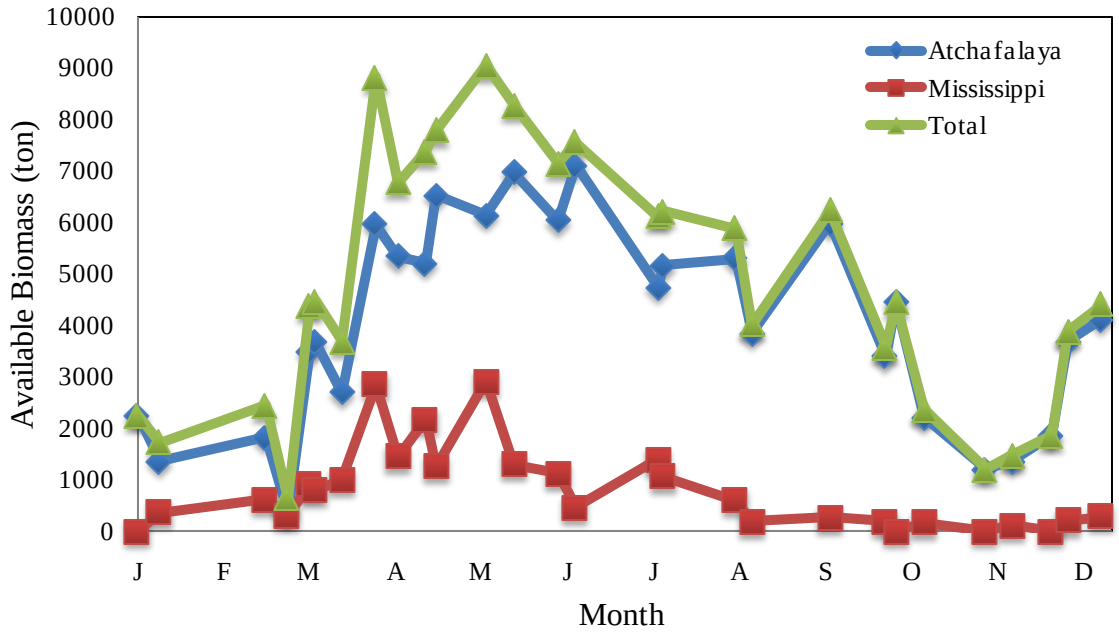

Figure 3-3. 2007 Atchafalaya region and Mississippi region estimated algal biomass.

3.2. Analysis of Harvesting Methods

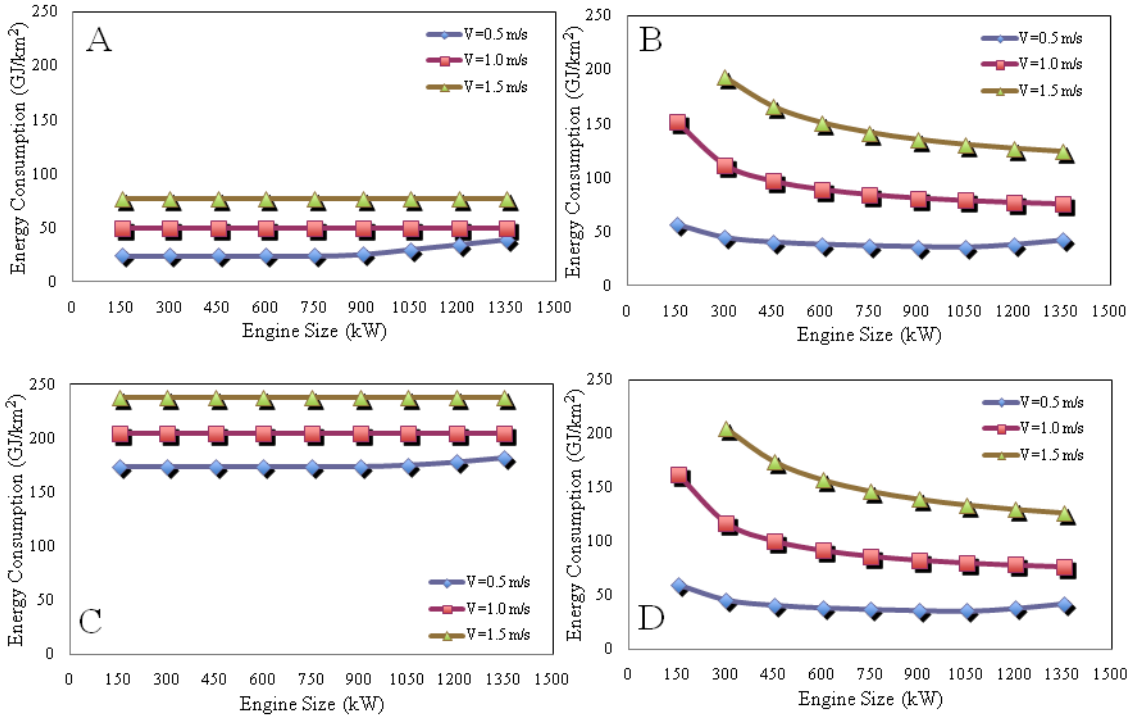

Figure 3-4. Harvesting vessel, technologies comparison; (A) Plankton net trawling, (B) Traveling screen with focusing arm, (C) Traveling screen only, (D) Screw pump filtration.

Figure 3-4 presents the energy consumption of harvesting 1 km^2 of ocean surface with different vessel engines at different speeds for four different harvesting methods. Graph A represents plankton net trawling, B is traveling screen with focusing arm, C is for a traveling screen only and D is for a screw pump with filter screen. We assumed the vessel engine is always operated at full load, with all engine power is used to overcome the total drag force resistance from the ship, harvesting equipment and focusing arm. Therefore, as the engine size increases or harvest speed decreases, the harvest width increases. Three different harvest speeds were tested. They are: 0.5 m/s, 1 m/s and 1.5 m/s. Based on Fisherman's Workbook (Prado, 1990), 0.5 m/s is the lowest reasonable cruise speed. In the northern Gulf of Mexico coast, the engine size of a fishing boat is in the range of 75 kW to 1450 kW (Lloyd's Register of Shipping, 1995). Assumes harvesting depth is 0.5 meters.

Our analysis showed that a larger engine size requires less energy for harvesting until the width of harvesting technique reaches a maximum limitation. Based on personal correspondence with an experienced fisherman (C. Y. Lin, personal communication, 23 May 2010), the width of a harvesting equipment should not be more than three times larger than the ship length or it will cause the boat to become unstable have difficulties when making turns. In general, the length of large steel trawlers is usually in the range of 30 to 42 meters (East Coast Marine, Manufacture). In our model, we assumed that the max ship length is 50 meters. Therefore the maximum harvest width is 150 meters. When using a large engine boat, although it can support a wider harvester width, the width should still be limited to 150 meters. We assume the boat is always operated at full loading. This assumption causes the fuel consumption to be somewhat overestimated, since it actually does the same work as a smaller engine. However, based on Edgar (2009), the engine energy efficiency is maximized at 100% loading and decreases while the engine loading reduced. Thus, the proper vessel engine size will be the minimum that allows the harvest width of 3 times the vessel length.

Figure 3-4 also shows the effect of harvest velocity. It is obvious that the slower harvesting speed consumes less fuel, due to faster vessels encountering more resistance per harvested area. Thus a faster vessel can only harvest a narrower area to cut down on resistance. Although the faster harvesting speed requires less time for harvesting per unit ocean surface, the resistance is

represented by a quadratic relationship with speed, and ends up extending the harvesting route and ultimately increasing the total energy consumption and overall harvesting time.

Comparing four different harvesting technologies, the minimum energy requirement for plankton net trawling is 25 GJ/km^2, whereas a traveling screen with focusing arm and screened screw pump had a slightly higher value of 38 GJ/km^2. The minimum energy requirement for traveling screen without focusing arm was 173 GJ/km^2. This result suggests that the focusing arm plays an important role in energy balance since it requires less energy per harvest area. There are two reasons to explain why plankton net trawling consumes less energy. First, the machinery energy consumption of harvesting with a plankton net is less than a traveling screen and screw pump. Second, the 10 μm mesh size has 6% open area. The open area decreases the resistance on net thus allowing the use of a wider net for harvesting at the same engine power.

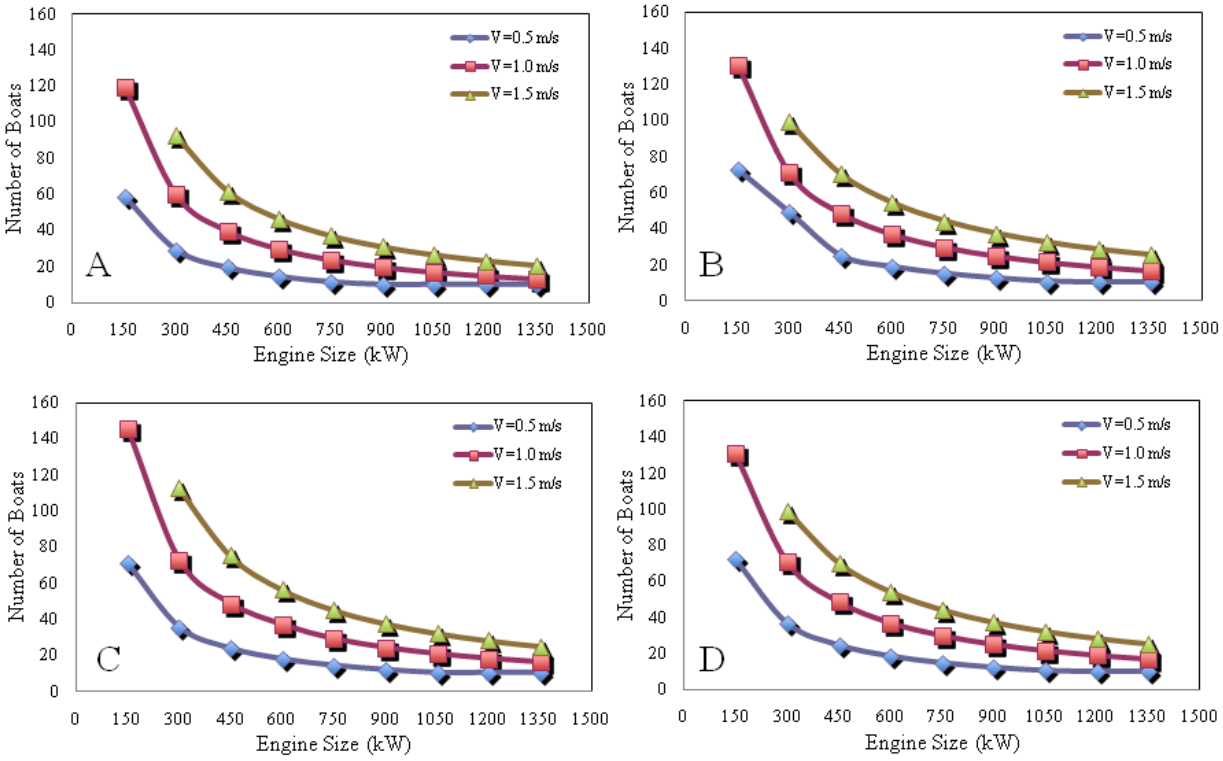

Figure 3-5. Number of Vessel Required to cover the Gulf of Mexico study area once a year; (A) Plankton net trawling, (B) Traveling screen with focusing arm, (C) Traveling screen only, (D) Screw pump filtration.

Figure 3-5 shows the number of vessels required to cover the whole study area once a year over different harvesting speeds and engine powers with different harvesting techniques. Results show that slow harvesting speeds require the least number of vessels. This is because a slower vessel can generally install wider harvest equipment. For plankton net trawling at 0.5 m/s, the number of required vessels approaches an plateau value after 750 kW. For traveling screen with and without focusing arm and screw pump, the number approaches an plateau value above 1050 kW. Therefore, considering the number of ships needed and energy consumption at different engine sizes, the proper engine size for plankton net trawling is between 750 to 900 kW at 0.5 m/s. For the other harvesting technologies, an engine size around 1050 kW is the best choice.

3.3. Harvest Depth

This section presents the relationship between harvest method, harvest depth and available biomass. It is important to judge the best harvesting depth and proper harvest methods since the algal bloom has a vertical distribution. By comparing the energy consumption and available biomass at different depths, we can decide the most efficient harvesting depth.

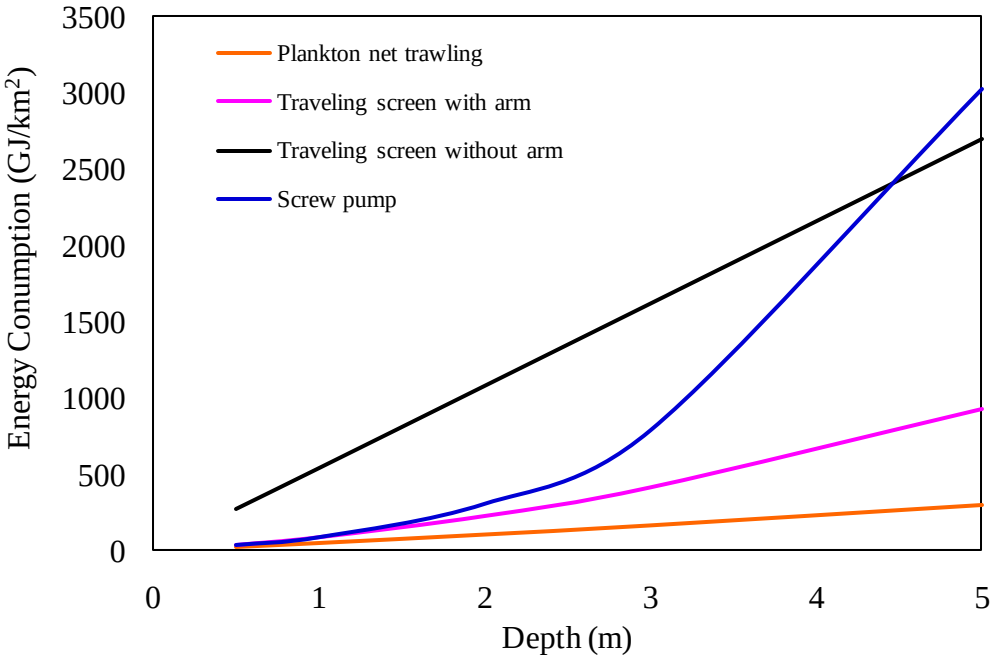

Figure 3-6. Relationship between harvest depth and harvest energy consumption of different harvesting techniques by HABER model.

Figure 3-6 compares the harvest energy consumption at different depths. The vessel size and harvest speed are optimized from previous results, which is plankton net trawling at 0.5 m/s on 750 kW vessel. The rest of the harvesting methods are conducted at 0.5 m/s on 1050 kW vessel. This result shows plankton net trawling is the best harvest method since it requires the least energy to harvest algal biomass at all depths. When harvesting deeper, the amount of water that is processed increases. Therefore, the machinery energy consumption for harvesting is increased with harvesting depth. The slope is different between the harvesting methods. The screw pump harvesting methods has a non-linear relationship between harvest depth and energy, because it pumps the water to a higher level when filtering more water.

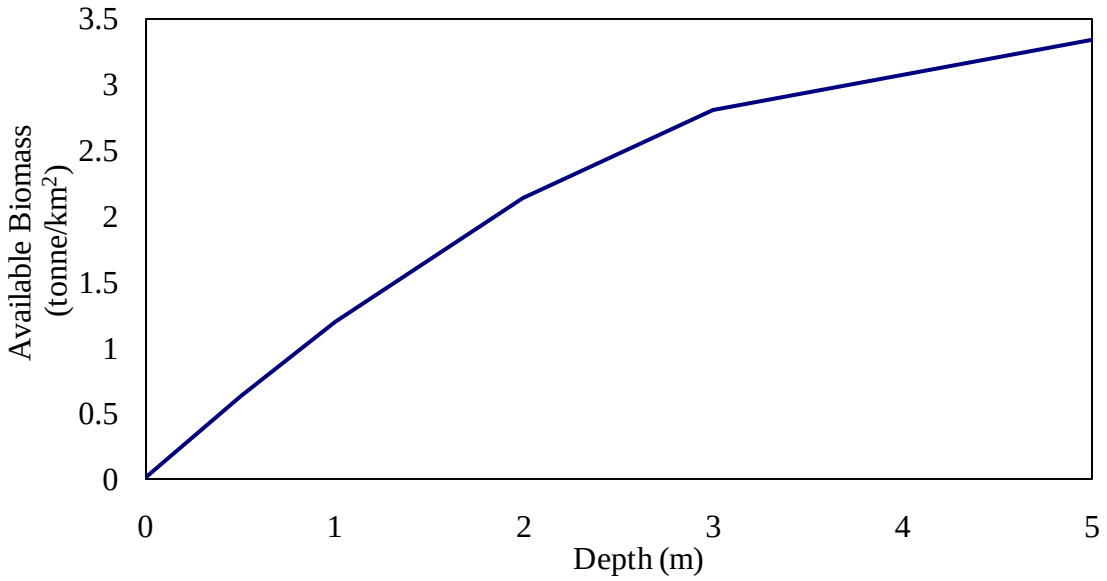

Figure 3-7. Simulation of accumulated algae biomass when harvest from surface to 5 m depth based on vertical distribution model.

Figure 3-7 shows the estimated average amounts of algal biomass available when harvesting from the surface to 5 meters depth at the area where chlorophyll concentration is 10 mg/m^3. For example, if harvesting from the surface to 2 meters depth, the total harvested biomass is 2 metric tons. This figure is estimated based on the vertical distribution model (See Section 2.2.2) and assumes the harvest area has a 10mg/m^3 chlorophyll concentration. Combining Figure 3-6 and Figure 3-7, the amount of algal biomass harvested per unit energy consumption at different depths can be calculated, which is shown in Figure 3-8.

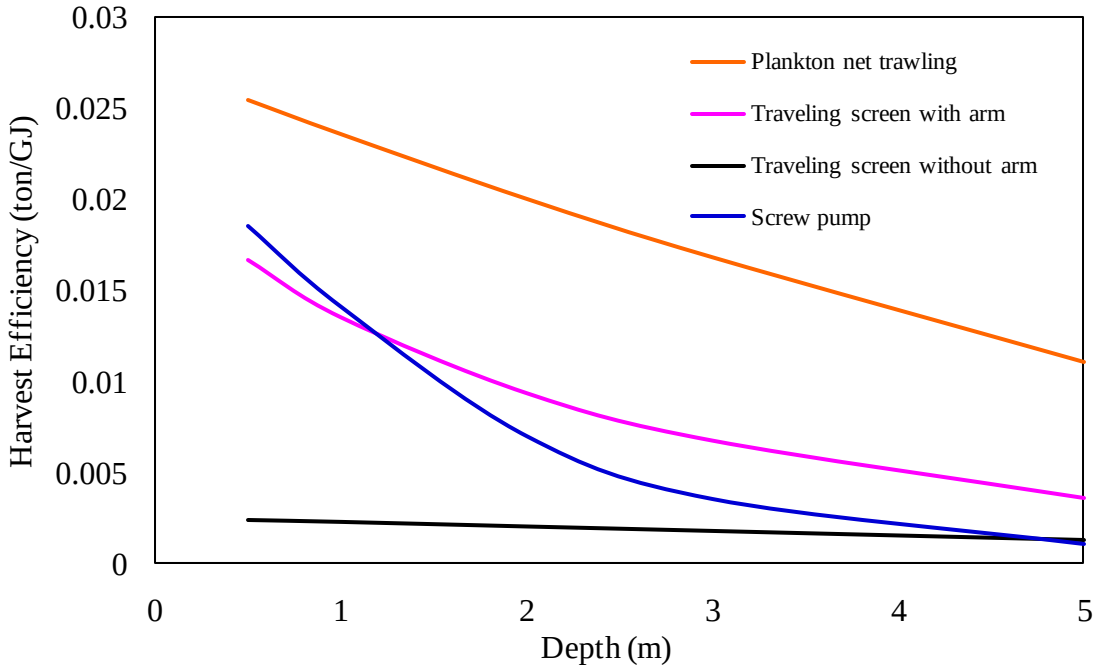

Figure 3-8. Harvest efficiency at different depth based on HABER model.

Figure 3-8 indicates that using plankton net trawling and harvesting from the surface to 0.5 meter depth is the most efficient method, it can harvest 25 kg dry biomass with 1 GJ energy input in the area that has 10 mg/m^3 chlorophyll concentration. The harvest efficiency decreases as harvest depth increases, and the best harvest depth was ultimately determined by the minimum harvest depth that was considered to be practical (0.5 m). With our modeling approach, the energy balance of the whole harvesting process, plankton net trawling at 0.5 m/s on 750 kW vessel and harvesting to 0.5 meters depth is the best condition. This result also highlights the potential advantages of combining harvesting methods with vertical focusing technologies like flotation, light attraction and others. With vertical focusing, the harvested biomass can be increased significantly without increasing the energy of the harvesting machinery.

3.4. Conversion Technologies Comparison

This section compares the net energy production of four different conversion technologies and estimates the biofuel production while processing different common algal species in the Gulf of Mexico.

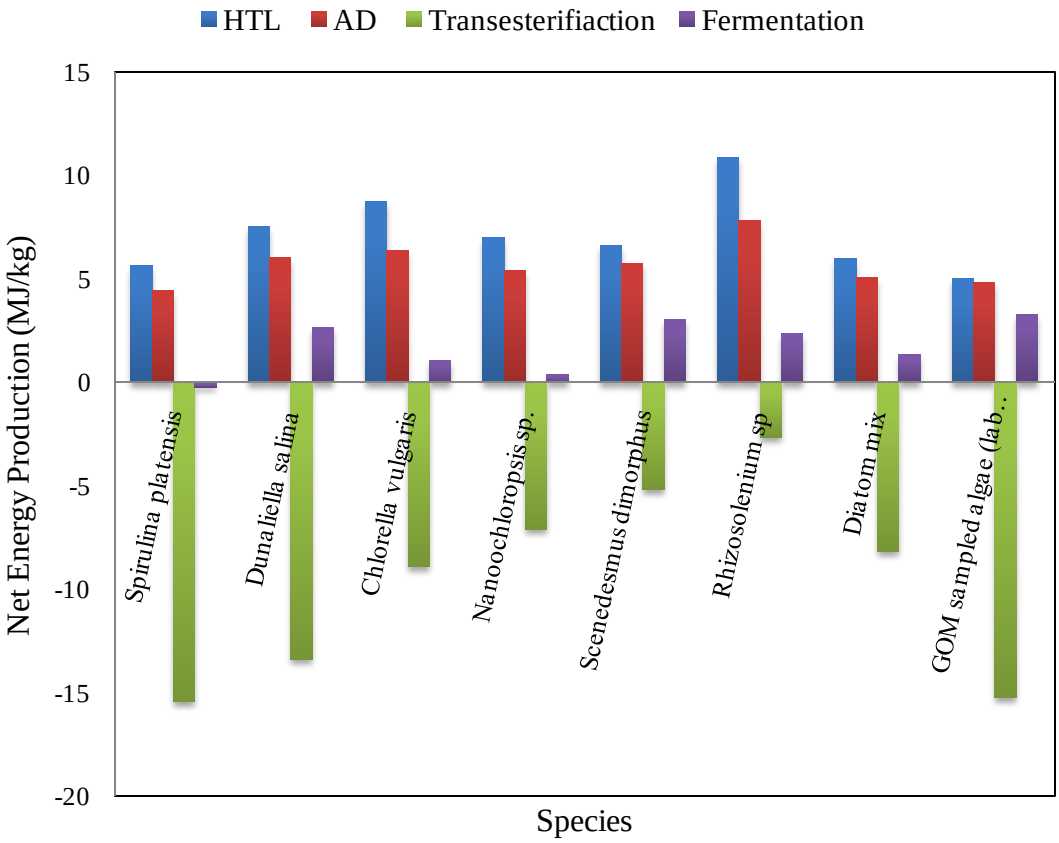

Figure 3-9. Biofuel net energy yield from different algal species.

Figure 3-9 presents the results of biofuel energy yielding from different biofuel conversion methods when using algal species as a feedstock. The estimation is based on the Biofuel Conversion Model introduced in the previous chapter, which is based on the algal biochemical composition is listed in Table 2-1 and previous experimental work on the relationship between biomass composition and conversion efficiency. From the figure, HTL and anaerobic digestion produce a positive energy balance with most types of algal feedstocks. This is because both HTL and AD are full cell body processing technologies. They transform larger portions of algae into biofuels rather than only the lipids or carbohydrates. HTL generally produces more energy than anaerobic digestion. However, the conversion factor we used in the HABER model for AD was 0.5, but literature report range from 0.3 to 0.7, depending on the reaction conditions and hydraulic retention times. Thus, the energy production of HTL and anaerobic digestion could actually be closer to each other, and further study is necessary to determine the most applicable value for this application. Even so, when the energy production is close between these two

techniques, HTL is still has the important advantage of faster processing time (minutes rather than days) and smaller reactors. Transesterification requires a large energy input because of the drying process. The biomass has to be dried to approximately 80 - 90% solid content for lipid extraction. Therefore, the key to making transesterification a positive energy balance is developing wet extraction methods. Fermentation has a similar challenge of related to a large energy input for distillation. Furthermore, algae in the Gulf of Mexico are generally low carbohydrate content species; fermentation can only convert carbohydrate into ethanol. Therefore, fermentation seems to be less practical for naturally harvested algal biomass.

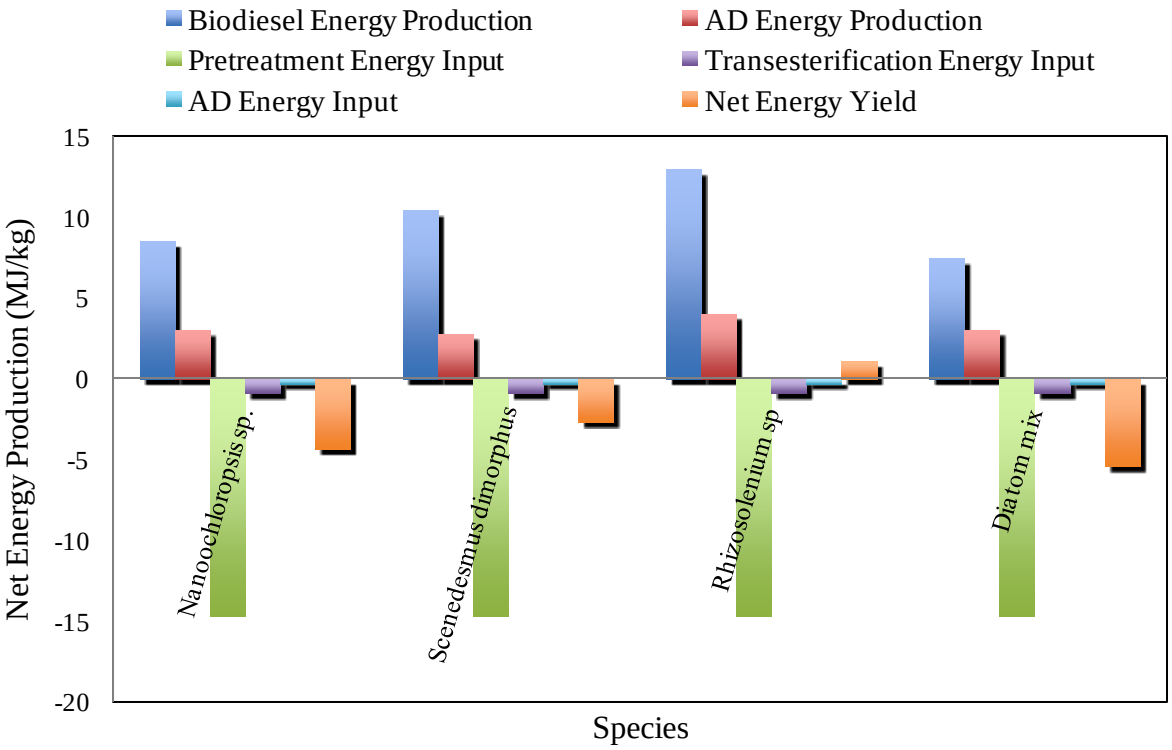

Figure 3-10. Energy production of anaerobic digestion/transesterification integrated process.

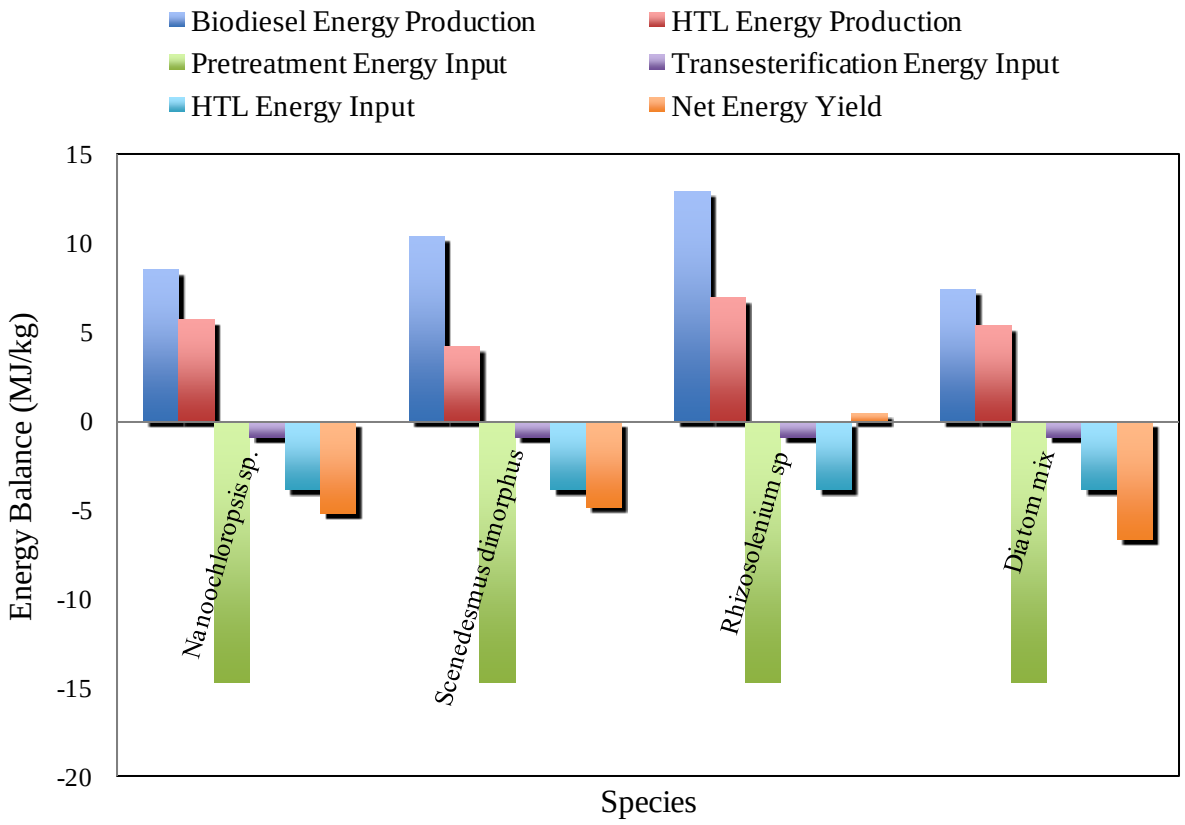

Figure 3-11. Energy production of HTL/transesterification integrated process.

Some researchers had stated the possibility and benefits of integrating different conversion process. For example, combining anaerobic digestion and transesterification together can convert lipids into biodiesel and convert extracted residue into biogas (Chisti, 2008). Figure 3-10 and Figure 3-11 presents the energy balance for integrated process of anaerobic digestion plus transesterification and HTL plus transesterification for a variety of potential algal feedstocks. The results show that both process combinations generate negative energy balance with most algal species. Only when processing a high lipid specie like *Rhizoslenium* sp., can the hybrid process produce a positive energy output. These results suggest that with current technologies, integrated conversion processes are not suitable for naturally harvested algae. Comparing all conversion processes in the model, HTL and anaerobic digestion are significantly more favorable than others in terms of energy yield.

3.5. Overview of Energy Consumption

According to the previous sections, preferable parameters were identified, for harvesting vessel engine size, harvesting speed, harvesting method, harvesting depth and conversion methods. This section uses these preferable parameters to evaluate the overall energy yield and identify desirable harvesting conditions in terms of chlorophyll concentration.

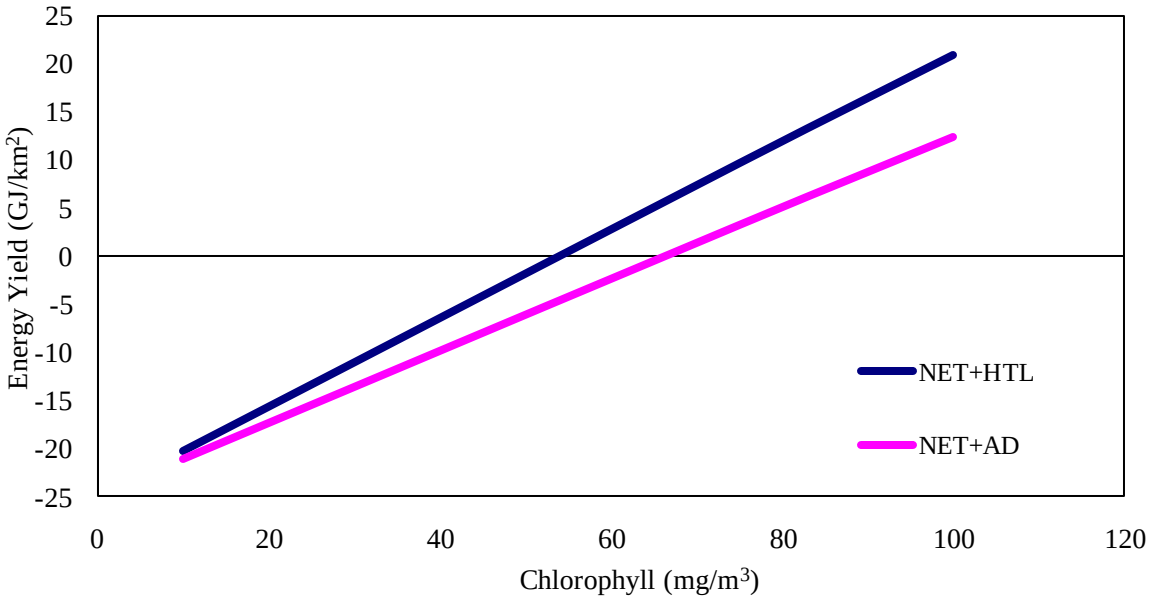

Figure 3-12. Overall energy balance of the two best combinations of harvesting and conversion process as a function of surface chlorophyll concentration based on the HABER model.

Figure 3-12 shows the relationship between chlorophyll concentration and overall energy balance. The parameters used in this test are based on the sections discussed above. The optimal condition is using plankton net trawling for harvesting algae at 0.5 meters depth and at 0.5 m/s speed on 750 kW fishing boat. Collected algae biomass is then processed though HTL or anaerobic digestion to produce crude oil or biogas. Available biomass is calculated by the vertical distribution model based on the given chlorophyll concentration. Assuming harvesting in the summer means that picoplankton is the dominant species. The energy consumption for harvesting per unit ocean surface area is fixed. The energy consumption for conversion is variable with the amount of processed biomass. Two scenarios: plankton net trawling with HTL(NET+HTL) and plankton net trawling with anaerobic digestion(NET+AD) are compared in the figure. The results indicate the energy break-even point for NET+HTL is at 55 mg/m^3

chlorophyll concentration, where the break-even point for NET+AD is 68 mg/m^3. 50~70 mg/m^3 chlorophyll concentration is equal to 6.3~9.5 g/m^3 biomass concentration. From previous literature, most algal blooms in the Gulf of Mexico have chlorophyll concentration around 40~50 mg/m^3 (Vargo, 2009). The only recorded value in excess of 100 mg/m^3 in the Gulf of Mexico was a red macroalgae Sargassum bloom that occurred in 2005. However, after the bloom in 2005, there has been no such bloom concentrations recorded (Gower et al., 2006).

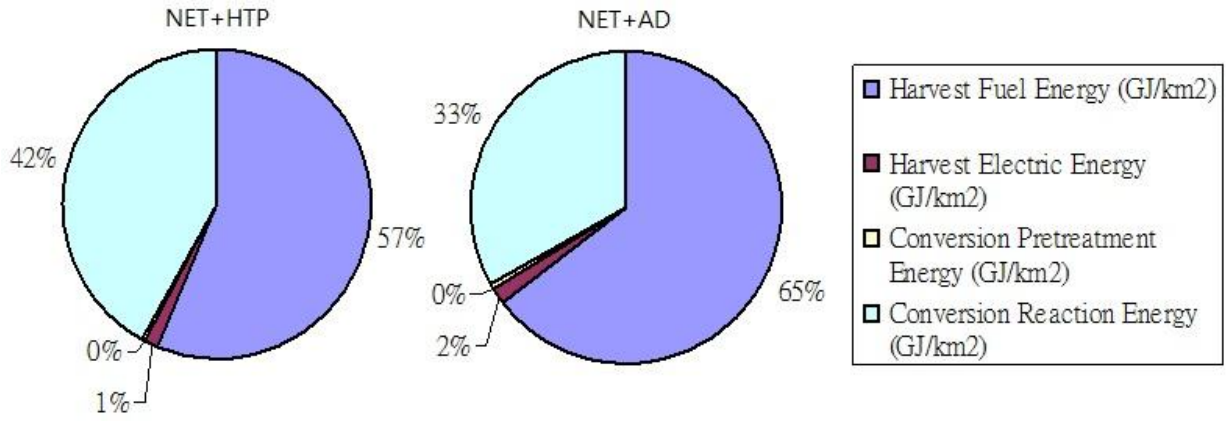

Figure 3-13. Energy consumption ratio of NET+HTL and NET+AD at break-even chlorophyll concentration.

Figure 3-13 is the energy consumption ratio at the break-even point. For both NET+HTP and NET+AD, harvest fuel energy consumption is the major energy input, 57% for NET+HTP, 65% for NET+AD. This result suggests that if we can reduce vessel fuel used for harvesting algae or convert to stationary algae harvesting, we can easily achieve a positive balance. For example, build a coastal station with a nutrient absorption media array that attracts algae growth on it. The only energy consumption for harvesting by this method would be scouring algae out of media. Figure 3-14 shows the energy balance of coast stationary algae cultivation, harvesting and conversion of biomass into biofuel. The estimation result shows the positive energy balance with chlorophyll concentrations in excess of 1 mg/m^3, which is equal to 126 mg/m^3 biomass density. Figure 3-15 shows the potential benefits of integrating a flotation system with net harvesting. A flotation system could focus vertical algal biomass up to the water surface (Bare et al., 1975). Phoochinda had studied the efficiency of removing algae from water through flotation (Phoochinda and White, 2003). In this model, flotation can help net harvesting with HTL achieve

the energy break-even point at 10mg/m^3 chlorophyll concentration, for AD this value becomes 13 mg/m^3.

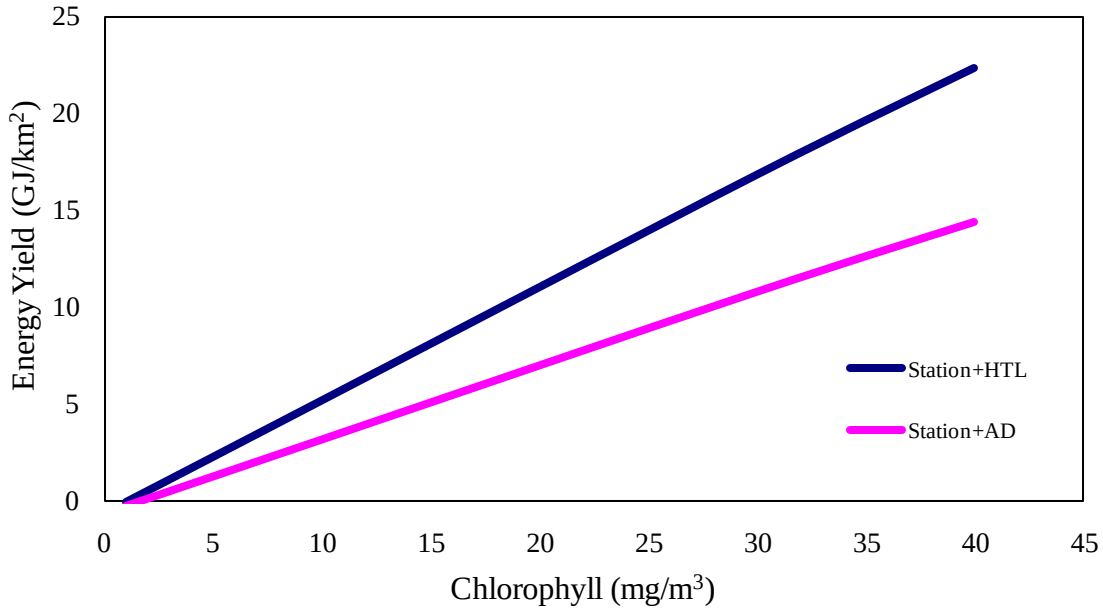

Figure 3-14. Overall energy balance of stationary harvest plus HTL or AD at different chlorophyll concentration.

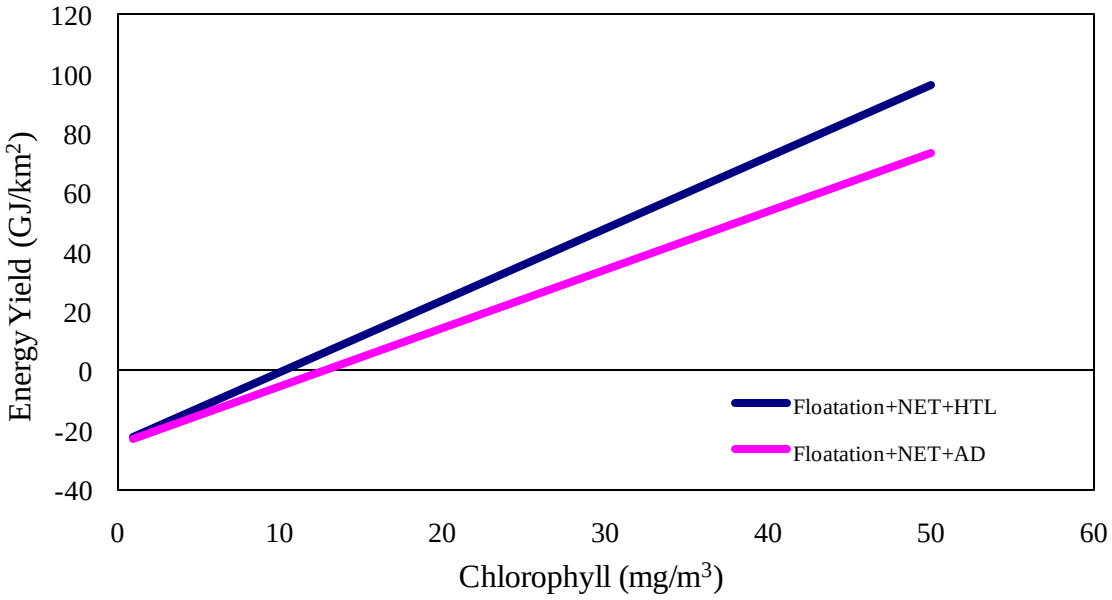

Figure 3-15. Overall energy balance of combination of flotation with net harvesting plus HTL or AD.

3.6. Sensitivity Analysis

The purpose of sensitivity analysis is to determine the variation of the model output by changing input parameters. In other words, it studies the model behavior in response to the variations of the input factors. It generates a range of effects due to an uncertain factor; thus providing higher credentials to the model. Sensitivity analysis is useful in mathematical models because it improves the understanding of the relationships between uncertainty in inputs and its outputs, which makes recommendation based on the model more credible.

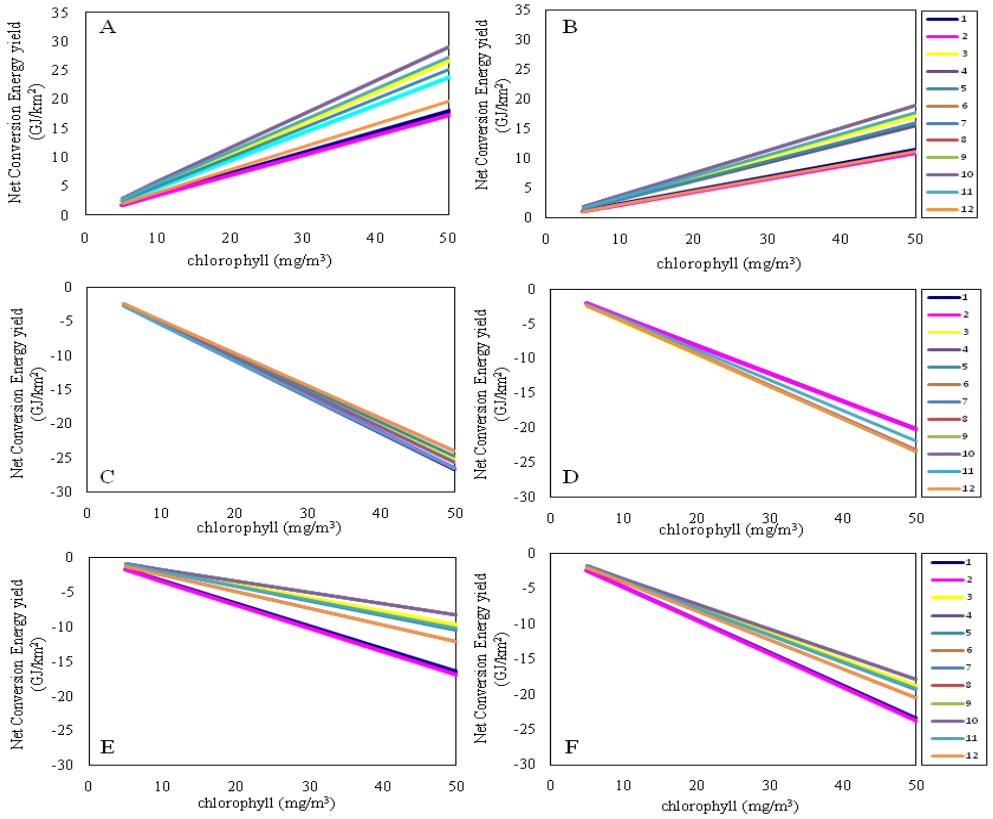

Figure 3-16. Sensitivity analysis of the impact of algal biomass at different month on net conversion energy yield, (A) HTP, (B) AD, (C) Transesterification, (D) Anaerobic digestion, (E) HTL+Transesterification, (F) AD+Transesterification.

Figure 3-16 shows the effects of variations in algal biomass harvested at different month presence to conversion net energy yield. The spread of spectrum is affected by the variation of algal biochemical components between species and conversion ratios.

HTL net conversion energy yield is between 17~29 GJ/km^2 when the field chlorophyll concentration is 50 mg/m^3. AD net conversion energy yield is between 11~19 GJ/km^2 when the field chlorophyll concentration is 50 mg/m^3. Both conversion methods have the highest yield on October and the lowest yield on February. Comparing the results between HTP and AD, HTP has wider spread than AD. Since both HTP and AD convert whole algae components, this result suggests HTP has higher overall components conversion rate than AD regarding the natural harvested algal biomass. Figure 3-16 also suggests that algal biomass in January, February and December produce less energy than other months. Diatoms and dinoflagellate are the dominant species in these three months, which means the biochemical composition of picoplankton is more favorable for HTL and AD process.

The range of net conversion energy yield of transesterification is between -24~ -26.6 GJ/km^2 when the field chlorophyll concentration is 50 mg/m^3. The energy yield of transesterification is relatively stable. This is due to the difference of algal biomass lipid content between different month is small, the lipid content at different month is between 16.02~ 18.29%. The range of net conversion energy yield of fermentation is between -20~ -23.3 GJ/km^2 when the field chlorophyll concentration is 50 mg/m^3. The small variation of net conversion energy yield of fermentation is because the small conversion coefficient.

Comparing the results of AD+Transesterification and HTL+Transesterification, HTL+Transesterifcation generates more energy than AD+Transesterfication. Since both processes combine with transesterifcation, the differences in the spread are actually caused by the differences in conversion rates of proteins and carbohydrates between HTL and AD. Therefore, the result shows that HTL has higher mixed conversion rate of proteins and carbohydrates than AD. In the first comparison, HTL has higher overall components conversion rates than AD. This result indicates HTL has higher lipid conversion rates or is less negatively affected by ash.

The sensitivity analysis reveals the range of biofuel energy production in different month and suggests that the algal biomass in January, February and December produce less energy through HTL and AD comparing to other months.

4. DEMONSTRATION EXPERIMENTS

4.1. Plankton Net Harvesting

From the HABER model, we concluded that the best harvesting technology is plankton net trawling. Considering the clogging time and algal cell size in the Gulf of Mexico, we selected 10 μm mesh size plankton net as the harvesting parameter. The algal cell size in the Gulf varies from a few microns to hundreds of microns. Diatoms, dinoflagellate are larger than 20 μm. However, in Rabalais' study, picoplankton contributed largely to the chlorophyll concentration and was dominant in the northern Gulf of Mexico from June to October (Rabalais et al., 2002). Study points out that picoplankton are only dominant in cell concentration, and the total biomass is usually dominated by diatoms (Dortch et al., 2001). It is important to study the filter efficiency of harvesting picoplankton with 10 μm plankton net and adjust the harvesting efficiency input value in the model if needed.

4.1.1. Objective

The objective of this experiment is to measure the harvest efficiency of harvesting picoplankton with 10 μm plankton net and estimates the harvest efficiency at different concentrations. This helps provide better estimation of harvest efficiency in HABER model.

4.1.2. Methods

Picoplankton species, *Nannochloropsis oculata* was ordered from Florida Aqua Farm. It was cultivated under constant light at 25 ^{o}C in f/2 fresh water medium.. Plankton net was purchased from General Oceanics, Inc. The net body is made of 10 μm mesh size Nytex. Total suspended solids (TSS) were measured to present the algal biomass concentration. The procedure follows 2540D standard method (SMC, 1997). Total suspended solids dried at 103-105 ^{o}C, approved by standard methods committee. 25 to 400 ml of algae suspension were vacuum filtered by Millipore HA filter paper (0.45 μm pore size) and placed on a weighted dish, then oven dried over night until the weight was stable.

Three levels of concentrations were tested. They were low concentration: 2.5 mg/L, medium concentration: 5 mg/L and high concentration: 10 mg/L. Each level of concentration was in triplicate to verify the correction of data. Therefore, a total 9 batches of experiments had been

conducted. We diluted the stock algae suspension into favorable concentrations. Each batch filtered 20L of prepared algae suspension and then collected biomass before and after plankton net filtration. The harvest efficiency can be calculated by Equation (29):

$$\text{Harvest Efficiency} = \frac{\text{Harvested Biomass}}{\text{Filtered Biomass}} \tag{29}$$

4.1.3. Results

Figure 4-1 shows the size *of Nannochloropsis oculata* under microscope. The size of *N. otulata* is between 3 to 6 μm.

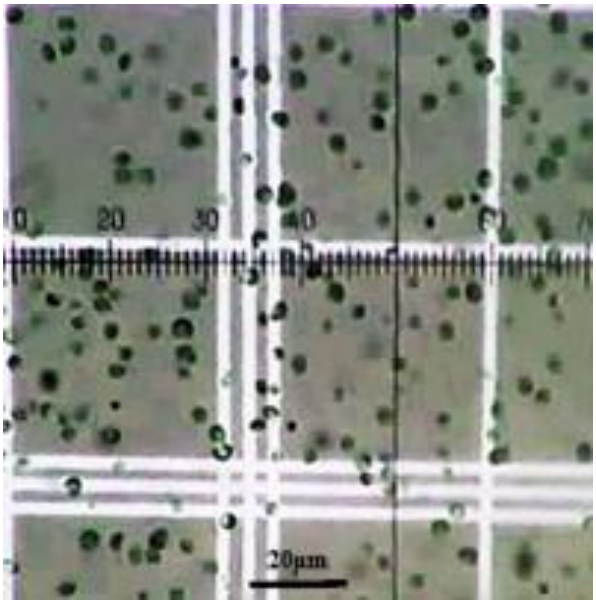

Figure 4-1. The size of *Nannochloropsis oculata* is verified by microscope.

Figure 4-2 shows the result of harvest efficiency test. There are only 8 data points since one low concentration sample dish was contaminated during drying. The result shows that harvest efficiency increases during concentration increases. The harvest efficiency is in the range of 5 to 70%. The linear regression fits best at R^2= 0.8291.

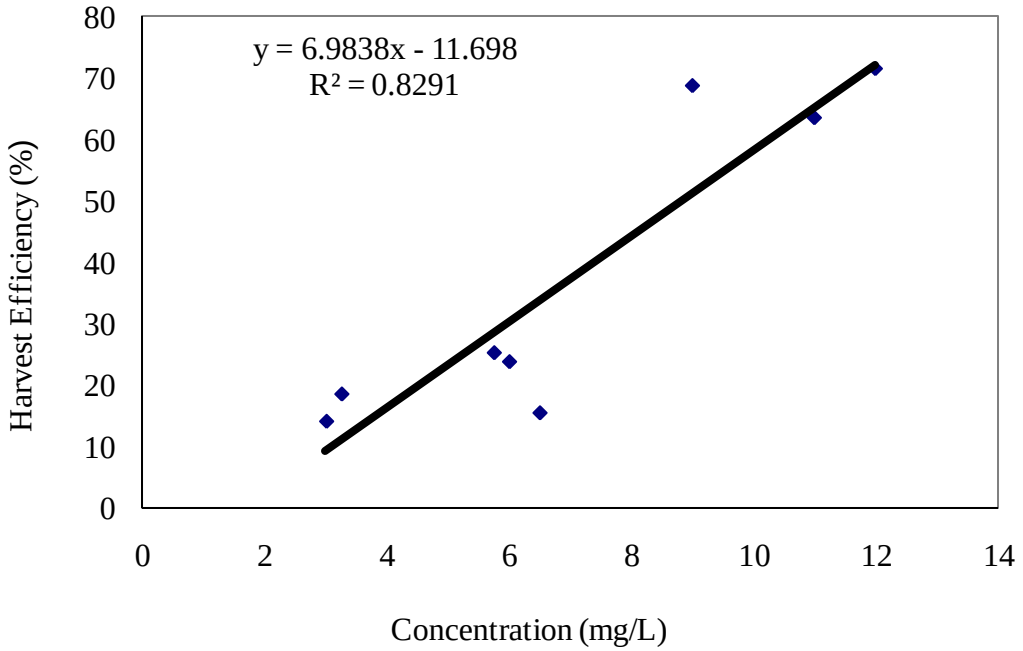

Figure 4-2. Harvest efficiency of *Nannochloropsis oculata* under different concentration using 10μm plankton net.

4.1.4. Discussion

During algal bloom, the chlorophyll density of water column can be as high as 60 mg/m^3, which is approximately equal to 7.2 mg/L biomass, taking 5 mg/L as average bloom density. The harvest efficiency is 20%, which is much lower than the assumed harvesting efficiency (80%). However, this test may underestimate the harvest efficiency because of the small processing volume. Model variables have to be adjusted by either changing harvesting mesh size or adjusting the expected harvest efficiency, especially in the period where picoplankton dominated the Gulf (June – October). Assuming the harvest efficiency for diatoms and dinoflagellates is 90%, and 20% for picoplankton, and considering the algae community composition across different months, the estimated harvest efficiency can be expressed in Figure 4-3.

Figure 4-3. 10μm plankton net harvesting efficiency at different month in the Gulf of Mexico.

4.2. Hydrothermal Liquefaction of Lab Cultivated Blue Green Algae

In HABER, the HTL crude oil production prediction model was based on the previous HTL experiment data of different algae species. However, Biller indicates that crude oil production prediction might be species specific since the differences in cell wall (Biller and Ross, 2010). Therefore, it is important to verify the effect of the model with respect to various natural algal species.

4.2.1. Objectives

To test the effectiveness of the crude oil production prediction model by using the Gulf of Mexico algae as feedstock and study the errors between experiment and model.

4.2.2. Methods

To obtain the local algae species from the Gulf of Mexico, we took Louisiana Universities Marine Consortium (LUMCON) cruise R/V Pelican, and went through two transects of the hypoxic zone for collecting algae sample in August 2009, shown as Table 4-4. Biomass samples were collected by 10 μm plankton net. Dissolved oxygen, chlorophyll data were recorded by CTD/Rosette System.

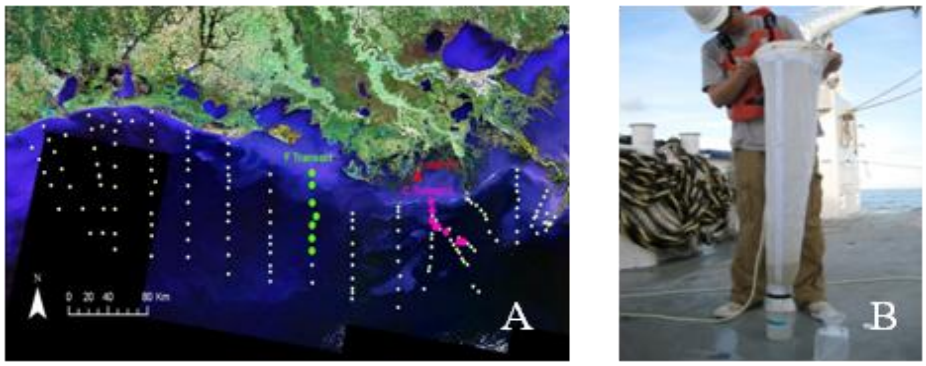

Figure 4-4. (A) Itinerary of the field trip, two transactions showed as green and pink dots; (B) Using Plankton net for collecting algae sample.

Collected algae samples were cultivated in our lab under light at 25^{o}C in f/2 medium. To collect sufficient biomass for HTL process, we scaled up the algae biomass in a step-wise method. A 3.5m^{3} inflatable swimming pool was used as an outdoor open pond cultivation reactor. Artificial seawater was prepared by Instant Ocean sea salt with f/2 media. The swimming pool was covered by clear a polyester sheet to limit environmental contamination. We harvestd algae with a flat sheet filter after the algae biomass concentration was in excess of 50 mg/L. Algae components were analyzed by Western Laboratory TEST 31.

The HTL process was performed according to previously reported methods (Dong, 2008). Solids content of the harvested algae sludge was adjusted to 20% dry matter before loading. The reaction condition is 280^{o}C, 30 minute reaction time. There was no catalyst used in this experiment. The crude oil sample was collected after the reactor cooled. The moisture content in the oil phase was determined by using a distillation apparatus based on ASTM Standard D95-99 (ASTM, 2004a). Solids residue content of the raw oil product was measured using Soxhlet extraction, according to ASTM Standards D473-02 (ASTM, 2004b) and D4072-98 (ASTM, 2004c).

Linear regression model was generated by the free statistic program R (ISM, 2008). Total 17 algal HTL data were used for production prediction model database. 11 algal HTL experiments data were provided by Dr. Zhang YuanHui's group in University of Illinois. However, these experiments were conducted with low lipid content (<6%) algal species, these data couldn't represent the correct coefficient of lipid converting into crude oil. Therefore, 6 literature data

from similar condition are included in the database. Table 4-1 shows the database used for HTL crude oil production modeling.

Table 4-1. HTL results.

Species	Crude Fat	Crude Protein	Carbohydrate	Ash	Crude Oil
Chlorella pyrenoidosa (HHC1)	2.30%	61.70%	21.70%	5.30%	38.70%
Spirulina plantensis (HHC2)	0.40%	68.30%	1.70%	9.50%	33.00%
Kelp (HHC3)	4.33%	5.46%	41.40%	21.40%	14.30%
PA051.1 green algae (API1)	1.30%	54.60%	16.10%	21.60%	47.40%
Agr-2n green algae (API2)	1.58%	19.50%	47.39%	4.75%	26.80%
Mixed species culture (ABE1)	0.10%	36.30%	9.13%	1.59%	37.90%
Mixed pond sample (YHZ1)	5.18%	5.60%	52.60%	49.60%	24.80%
UCSD wastewater sample	4.15%	33.60%	64.90%	9.95%	33.20%
Seaweed (AKG1)	5.60%	12.90%	41.30%	26.50%	6.80%
Chlamydonomas reinhardtii	3.80%	58.00%	1.00%	5.60%	35.60%
Red macroalgae	0.40%	21.50%	21.70%	41.60%	13.40%
aChlorella vulgaris	25.00%	55.00%	9.00%	11.00%	38.00%
[a]Nannochloropsis oculata	32.00%	57.00%	8.00%	3.00%	37.00%
[a]porphydium cruentum	8.00%	43.00%	40.00%	9.00%	21.00%
[a]spirulina plantensis	5.00%	65.00%	20.00%	10.00%	29.00%
[b]Botryococcus braunii	54.20%	20.60%	14.30%	10.90%	54.40%
[b]Dunaliella tertiolecta	2.87%	61.32%	21.69%	14.12%	35.70%

All units are the ratio of feedstock dry weight
a:(Biller and Ross, 2010)
b: (Sawayama et al., 1999)

4.2.3. Results

The result of linear regression model is shown in Table 4-2.

Table 4-2. Model: oil~lipid+protein+carbohydrate+ash+0.

	Estimate	Std. Error	T value	Pr(>|t|)
Lipid	0.66872	1.8263	3.662	0.002873**
Protein	0.41113	0.07656	5.370	0.000127***
Carbohydrate	0.30827	0.13759	2.240	0.043166*
Ash	-0.22511	0.21070	-1.068	0.304796

Signif. codes: 0 '***' 0.001 '**' 0.01 '*' 0.05 '.' 0.1 ' ' 1
Residual standard error: 0.1118 on 13 degrees of freedom
Multiple R-squared: 0.9003, Adjusted R-squared: 0.8696
F-statistic: 29.34 on 4 and 13 DF, p-value: 2.128e-06

The composition of algae sludge is shown in Table 4-3. The algal specie collected from the Gulf of Mexico appeared to be low lipid species. Table 4-4 shows the component proportions of the end products. Table 4-5 shows the difference between predicted values and experiment values. Experiment crude oil heating value is 20.36 MJ/kg.

Table 4-3. Gulf of Mexico sampled algae composition.

	Crude Protein(%)	Crude Fat(%)	Carbohydrate(%)	Ash(%)
Dry wt.	43.4	0.49	38.4	18.6

Table 4-4. HTL results.

	Refined Oil Yield(%)	Solid Residue(%)	Gas Yield(%)	Aqueous Product(%)
Dry wt.	29.6	16.07	21.63	32.64

Table 4-5. Difference of crude oil production between experiment and model.

	Experiment	Model	Difference (% of Exp.)
Dry wt.	29.6	23.0	-22.2
Heating value(MJ/kg)	20.1	34	69
Energy yield (MJ/kg)	5.94	8.82	23.9

4.2.4. Discussion

The linear regression model shows the coefficient of protein converting into crude oil through HTL is 0.41113, conversion coefficient of lipid is 0.66872, conversion coefficient of carbohydrate is 0.30827, and for ash is -0.22511. This result suggests lipid content is the major component affecting crude oil production. The R^2 of the prediction model is 0.90.

The biochemical composition analysis shows the algae species collected from the Gulf of Mexico contains almost zero lipid. Using HTL prediction model to predict crude oil production by the algal chemical composition and comparing the experiment results to prediction value. The variation in experimental value and value returned by prediction model is -22.2%. The difference of overall energy production between experiment and modeling value is 23.9%. This is because the crude oil heating value of tested algae is much lower than the assumption value 34 MJ/kg. It is still unclear why sampled algae have a lower heating value. Further research should address on how algal cell wall impacts the HTL crude oil production.

5. ECONOMIC AND ENVIRONMENTAL ANALYSIS

5.1. Economic Analysis

Three major costs are included in the economic analysis, they are: equipments cost, labor cost and fuel cost. Equipment cost includes the cost of purchasing vessels, harvesting equipments, conversion equipments and equipment installation. Labor cost is calculated by the assumption that five opertors on a fishing vessel and paid $15 per hour per operator (Payscale, 2010). Fuel cost is calculated based on the assumption that the harvesting vessel can run on the converted biofuels. Therefore, the fuel cost is the cost of purchasing extra fuel that cannot be covered by bioful.

To estimate the equipment cost of harvesting algae from the Gulf of Mexico, we include the cost of the vessel, harvesting equipment, conversion reactor and heat exchanger. The price of a used trawler is in the range of $50,000 to $500,000, depending on the size and condition (East Coast Marine, 2010). The membrane of the plankton net is the major cost component of the entire net. For 1 m^2 11 μm polyester screen the cost is $182. Assuming the filtered surface area is 4 times the net transaction area, 500 m^2 is sufficient for making two sets of plankton nets (Ecotao, 2010). Also, we assume half of the plankton net cost is equal to frame cost. A boiler is the closest common commercial reactor similar to HTL reactor. It can tolerate high temperature and high pressure. In the model, we assume harvesting 2 tons of dry algae biomass per km^2, which is equal to 10 tons of wet biomass for HTL. With a harvesting rate of 0.5 m/s, the time required to harvest 1 km^2 is 4.3 hr. Thus, the reactor loading is 5121 kg/hour. A heat exchanger costs $44,400 with double pipe construction. The exchange area is 1000 ft^2. Based on Douglas, the cost of equipment installation, pipeline, control system and electricity is about 95% of the equipment cost (Douglas et al., 1988).

Table 5-1. Equipments cost estimation.

Equipments	Price	Description	Sources
Fishing boat	500,000	Used trawler are in the range of 50,000 to 500,000. Engine size between 525 to 1050 kW	(East Coast Marine, 2010)
Plankton net	136,500	Polyester screen, 1 m^2 11um $182 assume 500 m^2 and 1/2 frame price	(EAS, 2009)
Boiler (reactor)	503,200	900F, 1500 psi oil fired	(Matches, 2010)
Heat exchanger	44,400	Double pipe, large 1000 ft^2 carbon steel, 900 psi	(Matches, 2010)
Other costs	1,124,895	Equipment installation, pipeline, control and electricity (95% of equipments price)	(Douglas, 1988).
Total equipments cost	2,308,995		

The other major cost is the fuel cost. Figure 5-1 shows the relationship of average chlorophyll concentration and the percentage of harvest fuel consumption offset by biofuel production. This figure suggests that if we harvest the algal bloom area where the chlorophyll concentration is excess 58 mg/m^3, the vessel fuel consumption can be fully offset by crude oil.

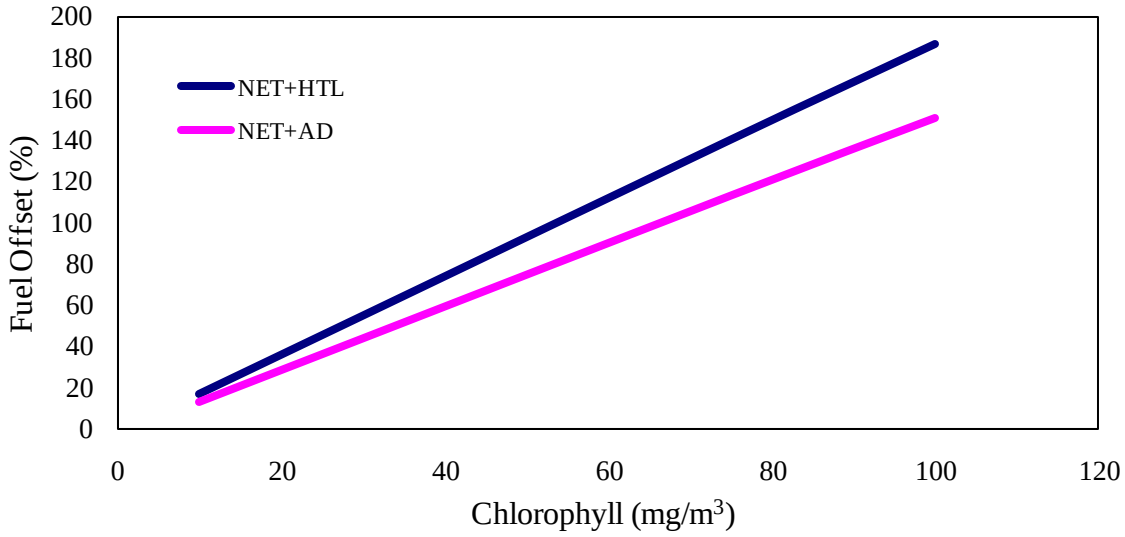

Figure 5-1. Fuel offset with different harvest density. NET+HTL offset 100% fuel consumption by biofuel production at 55 mg/m^3 and NET+AD achieves break-even point at 67 mg/m^3.

Figure 5-2 shows the monthly average of total algal biomass in high algal density area. In high density areas, average chlorophyll concentration is in excess of 7 mg/m^3. Figure 5-2 shows the monthly average of high algal density areas. It has been reported that the size of hypoxic area is closely related to the riverine nitrogen load in April, May June (Justic et al., 2002). Also, the satellite image analysis indicates April, May and June are the algal biomass peak months. Therefore, we conducted an economic analysis in these three months by using HABER.

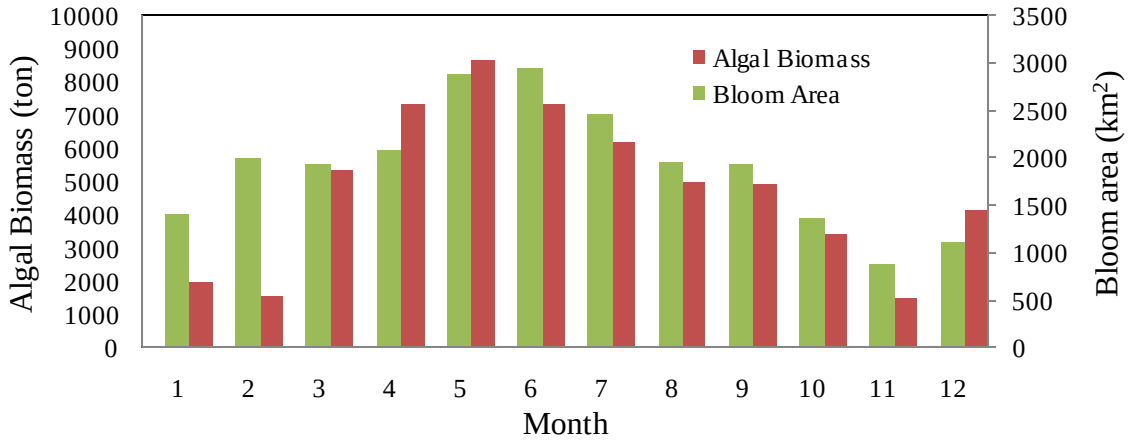

Figure 5-2. 2007 monthly average algal biomass and bloom area size in Atchafalaya and Mississippi Regions.

Table 5-2 estimates the total cost for April, May and June harvesting. In this analysis, we propose to harvest the target area once a month. Monthly average bloom area is the average area size in the northern Gulf of Mexico has chlorophyll concentration higher than 7 mg/m^3 from satellite images, in km^2. Monthly total biomass is the estimated total biomass in whole water column, calculated by the chlorophyll concentration, chlorophyll/biomass ratio and vertical distribution model. Monthly surface biomass is the amount of biomass from the surface to 0.5 meters depth. Monthly harvested biomass is the amount of biomass harvested from the surface to 0.5 meters depth with 10μm plankton nets, Figure 4-3 is used for adjusting harvesting efficiency. Biofuel net energy production is the net energy yield of harvested biomass by HTL process. Harvesting energy consumption is the energy consumed for harvest through the whole bloom area in each month. Assuming the fishing boat used in the model is powered by diesel engine and can run on the biofuel converted from algae. Fuel offset is the percentage of the energy content of the biofuel produced by harvested algae over the total fuel energy required for harvesting. For example, 100% offset means the boat can fully run on the biofuel from algae without buying extra diesel. Net fuel energy consumption is the difference between the total produced biofuel energy content and energy required for harvesting whole bloom area. Fuel cost is assuming the price of diesel is 3 dollar per gallon and 42 MJ/L (Pienkos et al., 2009), calculating the cost of fuel for harvesting energy consumption after biofuel offset. Number of vessel required is assuming to harvest bloom area once a month, and each boat works 12 hour and harvests 3 km^2 per day. Based on this assumption, the labor cost of a boat is $900 per day. Equipments cost is the cost of purchasing and installing equipments on boat. Total cost includes net fuel cost and equipments cost.

This analysis is based on the previously optimized conditions and adjusted with the harvest efficiency from Figure 4-3. Harvesting at 0.5 meters depth with 10 μm plankton net results in less than 10% of the total biomass being collected. The biocrude oil can offset the harvest fuel usage by 9.6%, 6% and 2.7% in April, May and June, respectively. The monthly fuel costs for harvesting are estimated at $3,687,584, $5,304,986, and $5,494,610. Considering the cost of the boat and labor cost, the total harvesting cost is $57,415,469, $80,056,826, and $82,582,445. Analyzes the total cost of harvesting with vertical focusing technology. The fuel offset becomes 98%, 85% and 72%, which is ten times higher than harvesting with plankton net only. The total cost of each month is $53,775,166, $75,617,608 and $78,685,887 in April, May and June.

According to these two tests, the major cost is equipments cost. With developing vertical harvesting technology, the fuel cost can be offset by 98% in April.

Table 5-2. Harvest cost in April, May June with basic technology.

Features	April	May	June
Monthly average bloom area (km^2)	2,075	2,870	2,941
Monthly total biomass (ton)	7309.7	8658.9	7344.5
Monthly surface (0.5m) biomass (ton)	1388.85	1645.18	1395.45
Monthly harvested biomass (ton)	708.31	608.71	279.09
Biofuel net energy production (GJ)	4947.5	4251.9	1949.6
Harvesting energy consumption (GJ)	51656.9	71448.4	71548
Fuel offset	9.6%	6%	2.7%
Net fuel energy consumption (GJ)	46709	67195	69598
Fuel cost ($)	3,687,584	5,304,986.8	5,494,610
Number of vessel required	23	32	33
Labor cost ($)	621,000	891,000	891,000
Equipments cost ($)	53,106,885	73,887,840	76,196,835
Total cost ($)	57,415,469	80,056,826	82,582,445

Table 5-3. Harvest cost in April, May, June with vertical focusing technology.

Features	April	May	June
Monthly average bloom area (km^2)	2,075	2,870	2,941
Monthly harvested biomass (ton)	7309.7	8658.9	7344.5
Biofuel net energy production (GJ)	51058	60482	51306
Harvesting energy consumption (GJ)	51656.9	71448.4	71548
Fuel offset (%)	98	85	72
Net fuel energy consumption (GJ)	599	10966	51306
Fuel cost ($)	47,282	865,768	1,598,052
Number of vessel required	23	32	33
Labor cost	621,000	864,000	891,000
Equipments cost ($)	53,106,885	73,887,840	76,196,835
Total cost ($)	53,775,166	75,617,608	78,685,887

5.2. Environmental Analysis

Based on Donald (2003), in order to reduce hypoxic zone area to 5000 km^2 to meet action plan's goal, riverine nitrogen loading should be reduced by 33% (EPA, 2007). The nitrogen loading to the Gulf of Mexico is 6000 ton/day (Donald et al. 2003). Therefore, we can estimate the environmental benefit by calculating the amount of algal biomass removal.

Table 5-4 shows the nitrogen removal by harvesting algae in peak season (April, May and June). Assuming 33 boats are used for harvesting, the harvest period is once every month. Here we also test the impacts of basic harvesting and harvesting with vertical focusing technology. The cost of harvesting in three months by plankton net trawling and by vertical focusing technologies is $93,357,016 and $81,380,937. Based on Veldhis (2005), the nitrogen content in algal biomass is usually between 5.8 ~ 11.6%. Therefore, the total nitrogen removal is between 92.5~185.15 metric tons for basic harvesting in three months. For harvesting with integrated vertical focusing, the nitrogen removal ranges from 1352.16~2704 metric tons. Comparing these numbers to nitrogen loading rate, we estimate 0.02~ 0.03% and 0.25~0.5% removal. Therefore, harvesting in high density areas could minimally affect hypoxia in the Gulf of Mexico.

Table 5-4. Nitrogen removal from algal harvesting.

Methods	Cost of Harvesting In Peak Season ($)	Biomass Removal (ton/90d)	Total Nitrogen Removal (ton/90d)	% of Nitrogen Loading
Basic harvesting	93,357,016	1596	92.5~185.15	0.02~0.03
Harvesting with vertical focusing	81,380,937	23313	1352.16~2704	0.25~0.5

6. CONCLUSION AND FUTURE WORK

This study has constructed the Harvest Algae for Biofuel Energy Recovery (HABER) model that has the capability to optimize operational variables, estimate the process outcome, and test the performance of various scenarios.

The annual available biomass in the northern of Gulf of Mexico has been estimated by the sea-WiFS satellite image, algae species composition and vertical distribution model. The biomass estimation is in the range of 800,000 metric tons to 200,000 metric tons, varying throughout the month. The estimated biomass in the Atchafalaya and Mississippi regions is between 600 and 9,000 metric tons.

Three different harvesting techniques and four scenarios were compared based on the Harvest Energy Consumption Model. First, we compared the impact of vessel engine size and harvest speed on harvesting energy consumption. The result suggests slow harvest speed (0.5 m/s) consumes less energy. The proper engine size is around 750 kW, with slight changes depending on the selected harvest equipments. We further compare the effects of harvest depth on energy consumption between different harvest scenarios. Harvesting by plankton net trawling requires the least energy. Considering the vertical distribution of algae, the harvest efficiency in terms of biomass collected per unit energy input (kg/MJ) can be calculated. At 10 mg/m^3 chlorophyll concentration area, plankton net can harvest 25 kg per 1 GJ energy input.

Biofuel Conversion Model (BCM) included four different common biofuel conversion technologies. To study the differences of biofuel production by processing different algae species, algal species biochemical compositions are entered into the model. The results suggest hydrothermal liquefaction and anaerobic digestion are more favorable in terms of energy production because they are whole cell processing reactions. Fermentation and transesterification have negative energy balances because they require higher energy input for distillation and drying biomass. Combining processes have also been tested by BCM. Transesterification combined with anaerobic digestion has been reported to be an improvement of transesterification. This study first tested the possibility of combining transesterification with HTL. The result of the test showed that combining these processes still produced negative energy

balance. Only one high nutrient algae species, *Rhizosolenium* sp, can generate a positive energy balance.

An overall energy consumption test revealed the preferable harvesting concentration that requires no extra energy input to the whole process. For plankton net trawling combining with HTL (NET+HTL), the break-even chlorophyll concentration is 55 mg/m^3. For plankton net trawling with anaerobic digestion (NET+AD), the break-even point is 68 mg/m^3 chlorophyll concentration. We further studied the portion of energy consumption during break-even point. For NET+HTL, 57% of energy consumption is vessel fuel usage, and 42% is conversion process. For NET+AD, 65% of energy consumption is attributed to vessel fuel usage, and 33% of energy consumption is in conversion process. Based on these results, we tested the possibility of stationary cultivation of algae in the ocean. The energy consumption test suggests that a positive energy balance with very low algal density. However, the cost of stationary cultivation and production of open ocean cultivation are the issues to be considered.

Two demonstration experiments were conducted to verify the uncertainty of the model. The first experiment was the picoplankton net filtration efficiency test. This experiment studied the relationship of picoplankton concentration to filtration efficiency. The 10 μm plankton net used in 5 mg/L biomass concentration had 20% filtration efficiency. Thus, the original variable in the model has to be adjusted according to monthly species community composition. The other demonstration experiment was the Gulf of Mexico lab cultured blue green algae HTL test. Testing the performance of HTL crude oil production prediction model. The result suggests that crude oil production can be higher than the prediction model. However, the experimental heating value is much lower than assumption used in the model. Therefore, the relationship of heating of crude oil and feedstock composition should have further research.

Economic analysis quantified the cost of the whole harvesting and conversion process. Basic harvesting technology and vertical focusing technology are compared in this study. Basic harvesting technology can harvest 1596 tons in 3 month for a cost of $93,357,016. Vertical focusing technology potentially could harvest 23313 tons in 3 month for a cost of $81,380,937. This result suggests that vertical focusing technology can offset 98% of harvesting fuel in April. The environment analysis shows harvesting natural occurring algae in Atchafalaya and Mississippi regions could minimally resolve the hypoxia problem. However, harvesting algae

with a fishing boat can effectively solve harmful algal bloom problems since it can capture algae in open-ocean and offset the fuel usage by converting biomass into biofuel.

It is possible to include novel harvesting or conversion technologies in the model and provide new results by inputting new parameters in the model. Also, HABER can be easily applied to other eutrophic areas like Great Lakes or Chesapeake Bay to determine the possibilities and energy output estimations of harvesting algae for biofuel in different locations by inputting site-specific algae characteristics.

.

REFERENCES

AVS. 2010. Harvesting, Dewatering and Drying. Marysville, OH.: AlgaeVenture Systems. Available at: www.algaevs.com/harvesting-dewatering-and-drying Accessed 08 September 2010.

Amon, T., B. Amon, , V. Kryvoruchko, A. Machmller. K. Hopfner-Sixt, V. Bodiroza, R. Hrbek, and J. Friedel. 2007. Methane production through anaerobic digestion of various energy crops grown in sustainable crop rotations. *Bioresource Technology* 98(17): 3024-3212.

Anderson, D., P. Glibert, and J. Burkholder. 2001. Harmful algal blooms and eutrophication: nutrient sources, composition, and consequences. *Estuaries and Coasts* 25(4): 704-726.

ASTM. 2004a. ASTM D95-99. Standard test method for water in petroleum products and bituminous materials by distillation. In *Annual Book of ASTM Standards*. West Conshohocken, PA: Am. Soc. for Testing Materials.

ASTM. 2004b. ASTM D473-02. Standard test method for sediment in crude oils and fuel oils by the extraction. In *Annual Book of ASTM Standards*. West Conshohocken, PA: Am. Soc. for Testing Materials.

ASTM. 2004c. ASTM D4072-98. Standard test method for toluene-insoluble (TI) content of tar and pitch. In *Annual Book of ASTM Standards*. West Conshohocken, PA: Am. Soc. for Testing Materials.

Barker, J. C. 2001. *Methane Fuel Gas from Livestock Wastes: A Summary*. Raleigh, NC.: North Carolina State University Cooperative Extension Service.

Bare, W., N. Jones, and E. Middlebrooks. 1975. Algae removal using dissolved air flotation. *Journal Water Pollution Control* 47(1): 153-169.

Bentz, A.P. 1997. Final Summary Report on Project 3310 Marine Diesel Exhaust Emissions (Alternative Fuels). Groton, CT.: United States Department of Transportation United States Coast Guard System.

Berglund, M., and P. Besson. 2006. Assessment of energy performance in the life-cycle of biogas production. *Biomass and Bioenergy* 30: 254-266.

Biller, P., and A. Ross. 2010. Potential yields and properties of oil from the hydrothermal liquefaction of microalgae with different biochemical content. *Bioresource technology* 102: 215-225.

Bohn, I., L. Brnsson, and B. Mattiasson. 2007. The energy balance in farm scale anaerobic digestion of crop residues at 11-37° C. *Process Biochemistry* 42: 57-64.

Brennan, L., and P. Owende. 2010. Biofuels from microalgae-A review of technologies for production, processing, and extractions of biofuels and co-products. *Renewable and Sustainable Energy Reviews* 14(2): 557-577.

Briand, X. 1997. Anaerobic digestion of Ulva sp. 1. Relationship between Ulva composition and methanisation. *Journal of Applied Phycology* 9: 511-524.

Burenin, V. 2002. Screw Pumps for the Oil Refining, Petrochemical, and Chemical Industries. *Chemical and Petroleum Engineering* 38(9-10): 532-537.

Booz, Allen and Hamilton, Inc., 1991, Inventory of Air Pollutant Emissions from Marine Vessels, Final Report. Los Angeles, CA.: California Air Resources Board.

CENR. 2000. *Integrated Assessment of Hypoxia in the Northern Gulf of Mexico*. National Science and Technology Council Committee on Environment and Natural Resources, Washington, DC.

Chisti, Y. 2008. Response to Reijnders: Do biofuels from microalgae beat biofuels from terrestrial plants? *Trends in Biotechnology* 26(7): 351-352.

Clarens, A. F., E. P. Resurreccion, M. A. White, and L. M. Colosi. 2010. Environmental Life Cycle Comparison of Algae to Other Bioenergy Feedstocks. *Environmental Sci. Technol.* 44: 1813-1819.

Dolan, J., G. Podnar, S. Stancliff, E. Lin, and J. Hosler. 2007. Harmful Algal Bloom Characterization Via the Telesupervised Adaptive Ocean Sensor Fleet. *In Pro.* 2007 NASA Science and Technologu Conference(NSTC-07). College Park, MD: EST.

Dortch, Q., N. Rabalais, R. Turner, and N. Qureshi. 2001. Impacts of changing Si/N ratios and phytoplankton species composition. *Coastal hypoxia: consequences for living resources and ecosystems* 1: 37-48.

Dong, R. 2008. Hydrothermal process for bioenergy production from corn fiber and swine manure. Ph.D. diss. Urbana, IL: University of Illinois at Urbana-Champaign, Department of Agricultural and Biological Engineering.

Dote, Y., S. Sawayama, S. Inoue, T. Minowa, and S. Yokoyama. 1994. Recovery of liquid fuel from hydrocarbon-rich microalgae by thermochemical liquefaction. *Fuel* 73(12): 1855-1857.

Dybas, C. L. 2005. Dead Zones Spreading in World Oceans. *Bioscience* 55 (7): 552-557.

EPA Science Advisory Board. 2007. Hypoxia in the Northern Gulf of Mexico. EPA-SAB-08-003. Washington, D.C.: EPA.

EPA Office of Transportation and Air Quality. 2000. Analysis of Commercial Marine Vessels Emissions and Fuel Consumption Data. Available at: http://www.epa.gov/orcdizux/models/nonrdmdl/c-marine/r00002.pdf. Accessed 06 May 2010.

Feinberg, D. 1984. Fuel options from microalgae with representative chemical compositions. Golden,Colorado.: Solar Energy Research Institute U.S. Department of Energy.

Fumento, M. Hypoxia Hype in the Gulf of Mexico. Nov. 12, 1999. Washington Times

Gladue, R. M., and J. E. Maxey. 1994. Microalgal feeds for aquaculture. *Journal of Applied Phycology* 6: 131-141.

Gröndahl, F. 2009. Removal of Surface Blooms of the Cyanobacteria Nodularia spumigena: A Pilot Project Conducted in the Baltic Sea. *Journal Information* 38(2): 79-84.

Hirano, A., R. Ueda, S. Hirayama, and Y. Ogushi. 1997. CO_2 fixation and ethanol production with microalgal photosynthesis and intracellular anaerobic fermentation. *Energy* 22(2-3): 137-142.

Hossain, A., A. Salleh, A. Boyce, P. Chowdhury, and M. Naqiuddin. 2008. Biodiesel fuel production from algae as renewable energy. *American Journal of Biochem. and Biotechnol.*4(3): 250-254.

Hwang, S. C. 1984. *Applied Trawler Equipments and Methods*. Beijing, China. I-non Publication.

Inoue, S., Y. Dote, S. Sawayama, T. Minowa, T. Ogi, and S. Yokoyama. 1994. Analysis of oil derived from liquefaction of Botryococcus braunii. *Biomass and bioenergy* 6(4): 269-274.

Justic, D., and N. Rabalais, R. Turner. 2002. Modeling the impacts of decadal changes in riverine nutrient fluxes on coastal eutrophication near the Mississippi River Delta. *Ecological Modelling* 152: 33-46.

Lamon, M. 1996. Method for harvesting brine shrimp cysts. *US Patent 5,513,462*.

Lardon, L., A. Hélias, B. Sialve, J. Steyer, and O. Bernard. 2009. Life-Cycle Assessment of Biodiesel Production from Microalgae. *Environmental Science & Technology 43*(17): 6475-6481.

Lavens, P., and P. Sorgeloos. 1996. *Manual on the production and use of live food for aquaculture*, Ghent, Belgium. Laboratory of Aquaculture and Arternia Reference Center.

MacFadyen, A. 1999. Modeling primary productivity from satellite-derived chlorophyll in the Monterey Bay region. Intent Papers of The Monterey Bay Aquarium Research. MBARI.

Lloyd's Register of Shipping . 1995. 1995 Lloyd's Register of Shipping. London, United Kingdom.: Marine Exhaust Emissions Research Program.

Mata, T., A. Martins, and N. Caetano. 2010. Microalgae for biodiesel production and other applications: A review. *Renewable & Sustainable Energy Reviews* 14(1): 217-232.

McCarl, B., and F. Boadu. 2009. Bioenergy and US Renewable Fuels Standards: Law, Economic, Policy. *Drake J. Agric. L*. 14: 43-74.

McClain, C. 2009. A Decade of Satellite Ocean Color Observations. *Annual Review of Marine Science* 1: 19-42.

McCormick, and Barnes W. 1979. *Aerodynamics, Aeronautics, and Flight Mechanics*. New York, N.Y. Wiley and Sons.

Mei, F., M. Dudukovic, M. Evans, and N. Carpenter. 2005. Mass and Energy Balance for a Corn-To-Ethanol Plant. St. Louis, MO. Washington University in St. Louis.

Mei C., H. Park, R. Sabzikar R, C. Qi, C. Ransom, and M. Sticklen. 2009. Green tissue-specific production of a microbial endo-cellulase in maize (*Zea mays* L.) endoplasmic-reticulum and mitochondria converts cellulose to fermentable sugars. *J. Chem. Technol. Biotechnol.* 84: 689–695.

Minowa, T., S. Yokoyama, M. Kishimoto, and T. Okakura. 1995. Oil production from algal cells of Dunaliella tertiolecta by direct thermochemical liquefaction. *Fuel* 74(12): 1735-1738.

Møller, H., I. Lund, and S. Sommer. 2000. Solid-liquid separation of livestock slurry: efficiency and cost. *Bioresource technology* 74: 223-229.

Morand, P., and X. Briand. 1999. Anaerobic digestion of Ulva sp. 2. Study of Ulva degradation and methanisation of liquefaction juices. *Journal of Applied Phycology* 11(2): 164-177.

Parry, M., O. Canziani, and J. Palutikof. 2007. *Climate Change 2007: Impacts, Adaptation and Vulnerability*. Intergovernmental Panel on Climate Change: Working Group II.

Patil, V., K. Tran, and H. Giselrød. 2008. Towards sustainable production of biofuels from microalgae. *International journal of molecular sciences* 9(7): 1188-95.

Peterson, A., F. Vogel, and R. Lachance. 2008. Thermochemical biofuel production in hydrothermal media: A review of sub- and supercritical water technologies. *Energy Environ Sci.*1: 32-65.

Phoochinda, W., and D. White. 2003. Removal of algae using froth flotation. *Environmental Technology* 24(1): 87-96.

Pienkos, P. 2009. The promise and challenges of microalgal-derived biofuels. *Biofuels, Bioprod. Bioref*. 3: 431-440.

Platon, E., B. Sen Gupta, and N. Rabalais. 2005. Effect of seasonal hypoxia on the benthic foraminiferal community of the Louisiana inner continental shelf: The 20th century record. *Marine Micropaleontol* 54(3-4): 263-283.

Prado, J., 1990. *Fisherman's Workbook*. Sete, France.: Food and Agriculture Organization of United Nations.

Rabalais, N., R. Turner, Q. Dortch, and D. Justic. 2002. Nutrient-enhanced productivity in the northern Gulf of Mexico: past, present and future. *Hydrobiologia* 176: 39-63.

Riffat, R., and K. Krongthamchat. 2007. Anaerobic treatment of high-saline wastewater using halophilic methanogens in laboratory-scale anaerobic filters. *Water Environment Research* 79(2): 191-198.

Samson, R., and A. Leduy. 1986. Detailed study of anaerobic digestion of Spirulina maxima algal biomass. *Biotechnol Bioeng*. 28: 1014-1023.

Sander K., and G. S. Murthy. 2010. Life cycle analysis of algae biodiesel. *The International Journal of Life Cycle Assessment* 15: 704-714.

Sawayama, S., T. Minowa, and S. Yokoyama. 1999. Possibility of renewable energy production and CO2 mitigation by thermochemical liquefaction of microalgae. *Biomass and Bioenergy* 17(1): 33-39.

Schenk, P. M., S. R. Thomas-Hall, E. Stephens, U. C. Marx, J. H. Mussgnug, C. Poston, O. Kruse, and B. Hankamer. 2008. Second generation biofuels: high-efficiency microalgae for biodiesel production. *Bioenergy Research* 1(1): 20-43.

Sheehan, J., T. Dunahay, J. Benemann, and P. Roessler, 1998. A look back at the U.S. Department of Energy's aquatic species program—biodiesel from algae. Report NREL/TP-580-24190 prepared by National Renewable Energy Laboratory, Golden, CO.

Sialve, B., N. Bernet, and O. Bernard. 2009. Anaerobic digestion of microalgae as a necessary step to make microalgal biodiesel sustainable. *Biotechnology Advances* 27(4): 409-416.

Smith, P., R. Counts, and R. Clutter. 1968. Changes in filtering efficiency of plankton nets due to clogging under tow. *ICES Journal of Marine Science* 33(2): 232-248.

Stumpf, R., and Tomlinson, M. 2005. Remote sensing of harmful algal blooms. In *Remote Sensing of Coastal Aquatic Environments*, 277-296. AH Dordrecht, The Netherlands: Springer.

Sylvan, J. B., Q. Dortch, D. M. Nelson, A. F. M. Brown, W. Morrison, and J. W. Ammerman. 2006. Phosphorus limits phytoplankton growth on the louisiana shelf during the period of hypoxia formation. Environmental Science and Technology 40(24): 7548-53.

Tsukahara, K., and S. Sawayama. 2005. Liquid fuel production using microalgae. *J Jpn Petrol Inst*. 48(5): 251–259.

Turner, R., N. Rabalais, and D. Justic. 2008. Gulf of Mexico hypoxia: Alternate states and a legacy. *Environmental Science and Technologies* 42: 2323-2327.

Tyedmers PH, Watson and R, Pauly D. 2005. Fueling global fishing fleets. Ambio 34(8):635-8.

Uellendahl, H., G. Wang, H. Moeller, U. Joergensen, I. Skiadas, H. Gavala, and B. Ahring. 2008. Energy balance and cost-benefit analysis of biogas production from perennial energy crops pretreated by wet oxidation. *Water Science & Technology* 58(9): 1841-1847.

Vargo, G. 2009. A brief summary of the physiology and ecology of Karenia brevis Davis red tides on the West Florida Shelf and of hypotheses posed for their initiation, growth, maintenance and termination. *Harmful Algae* 8: 573-584.

Ventikos, N., E. Vergetis, N. Psaraftis, and G. Triantafyllou. 2004. A high-level synthesis of oil spill response equipment and countermeasures. *Journal of hazardous Materials* 107: 51-58.

Vijayaraghavan, K., and K. Hemanathan. 2009. Biodiesel Production from Freshwater Algae. *Energy Fuels* 23: 5448-5453.

Walker, N., and N. Rabalais. 2006. Relationships among satellite chlorophylla, river inputs, and hypoxia on the Louisiana Continental shelf, Gulf of Mexico. *Estuaries and Coasts* 29(6): 1081-1093.

White, R. 1980. The Role of Liquid--Solid Separation in Today's Livestock Waste Management

Systems. *Journal of Animal Science* 50: 536-539.

Yang, Y., C. Feng, Y. Inamori, and T. Maekawa. 2004. Analysis of energy conversion characteristics in liquefaction of algae. *Resources, Conservation and Recycling* 43(1): 21-33.

Yen, H., and D. Brune. 2007. Anaerobic co-digestion of algal sludge and waste paper to produce methane. *Bioresource Technology* 98: 130-134.